POLYTECHNIC of TURIN

Energy Department

I Faculty of Engineering - Doctorate School
Doctoral of Philosophy in Energetics - XXXVII cycle

PhD Thesis

Design and modelling an innovative SOEC stack

Supervisor:

prof. Massimo Santarelli

Candidate:

Valerio Novaresio

April 2015

A VOLTE IL MODO MIGLIORE DI RISOLVERE I PROBLEMI
CONSISTE NEL RIMUOVERE I PROBLEMI STESSI

Il mio grazie va ai colleghi che in questi anni mi hanno supportato, incoraggiato e spronato ad arrivare fino in fondo.

Un grazie particolare, semplicemente per tutto, a colei che ieri era la mia musa, oggi è la mia fidanzata e domani sarà la mia sposa.

SOMETIMES THE BEST WAY TO SOLVE THE PROBLEMS
IS TO REMOVE THEM

My thanks to all the colleagues that in these years have supported, encouraged and spurred me to reach the end.

Special thanks, simply for everything, to her who yesterday was my muse, today is my girlfriend and tomorrow will be my bride.

III

Preface

The present work is focused on the design of a solid oxide cell stack that mainly works in electrolysis mode. The framework of the activity is the energetic issue related to the renewable sources management and storage capabilities. The analysis starts observing the energetic issue from an alternative standpoint that emphasizes the ethical aspects and instills in the reader the secondary importance of the efficiency respect to the feasibility and the robustness of the devices.

In order to predict the stack performance, a new numerical solver has been developed based on open source tool. This multi-physic solver can handle complete SOC stack both in fuel cell mode and in electrolysis mode. As a part of this activity an insight concerning SOC Electrochemical Impedance Spectroscopy physical simulation has been done. This part of the solver can be coupled with additional plugins and provides the basis for the impedance analysis of the low frequency part of the SOC spectrum. Basing on pragmatic approach a new stack design was proposed and technical drawings have been released. The stack is based on tubular cells considering some peculiarity of the planar configuration especially concerning charge transfer between electrodes and external current takes. Some simulations have been run in order to validate the main assumptions of the design process.

Keywords: SOC, OpenFOAM, EIS, stack design, modeling.

Index

Outline

In the present PhD thesis the design and modeling approaches to the development an innovative Solis Oxide Electrolysis Cell (SOEC) stack are presented. The reader starts from some background energy description and from some SOEC general description, then move inside the numerical part of the thesis and finally reach the design part in witch details of the innovative architecture are described.

In Chapter 1 a general description of the energetic framework is presented. Energetic needs are outlined and the relevant issues are described also concerning philosophical and ethical aspects. Particular emphasis was put in order to stress that technological innovations often can mean ethical progresses. In this context the crucial role cover by the energy storage was presented.

In Chapter 2 the reader can become familiar with SOEC devices and a thermodynamic description of high temperature electrolysis was made. SOEC are also analyzed in term of economical fluxes and some realistic chains were presented stressing on their feasibility both in economic and technical terms.

In Chapter 3 the reader get in the core part of the thesis. At the beginning the perimeter of the physical model was outlined and detailed description of mathematical models and numerical methods are presented. Particular emphasis was put in the description of the numerical code development (OpenFOAM®) both for what concern steady state and transient solver for deign point and polarization study and for what concern Electrochemical Impedance Spectroscopy (EIS) modeling. In particular an innovative and hybrid approach for EIS modeling was presented and detailed.

In Chapter 4 the second core part of the thesis was reported and an analysis of the critical issues of the state of the art technology was described. Starting from these considerations an innovative SOEC stack was proposed focusing both on technical and economic aspects. Some numerical results are showed and a detailed description of the stack, including technical draws and related bill of materials was reported.

In Chapter 5 some conclusions are put in order to summarize the work done. Mainly a recap of the main concepts, ideas and innovations were recalled. Additional remarks and some considerations for future works were then reported to link this thesis with possible new research projects.

Chapter 1
Energy Storage – Needs and limitations

The energetic issues

Energy is all. Everything one can think uses energy and the most important mankind evolution steps are related to the discovery of some innovative energy sources or to new energy utilization methods. The real primary energy source comes from stars nuclear reactions and further backlinks investigations concern the extremely advanced physic research area, or are related to ancient philosophical and religious questions. All mankind history is a continuous following one into another of acts, treaties or wars finalized to the energy control [1].

At the very beginning mammals have dominated reptiles due to their capacity to biologically store and use chemical energy. In the same way, many millennia later, the agriculture marked the beginning of the urban aggregation and the birth of kingdoms and empires. From the energy point of view agriculture and breeding represent respect to gathering and hunting a great innovation. In fact the energy density of a generic meter square of field has been significantly increased and the mankind has learned to store energy of the sun inside wheat, rice and corn in order to use it when required. Peoples have started to control such energy production and processes and as a consequence this has become the first driver for all the wars [2].

Other forms of energy previously stored in millions of years such as oil and coal, were neglected for long times because in general there was a huge imbalance between supply and demand. If we revisit the definition of renewable energy sources we can say that a source can be considered renewable if the time scale of the source depletion is higher compared to the time scale of the source production. In this sense until few centuries ago all energy sources can be considered renewables and only the food has represented the real energy issues. So it is not surprising that in the past, and not only in the past, the greater was the domination on the food sources the greater was the power that an empire or a kingdom held.

Power and domination are strictly related to energy control. The history teaches us that all the most powerful empires or nations have combined the capability to control large amount of energy sources and the capability

to store them. A nation can acquire power and hegemony respect to other nations if there is a global imbalance between energy demand and energy availability. The energy control is probably the most powerful instrument of a nation. For a nation or an empire the only other thing that has the same importance is the ability to issue money [3].

Energy transfers and energy market nowadays considerably increase their importance. In this sense electricity represents a very good way in order to exchange energy. In fact, after the necessary infrastructure have been built, electricity can be bought or sold very easily and with limited losses. In addition the sellers can have a robust control and dominance respect to the buyers because the electricity supply can be cut off very quickly.

The ethical matter related to energy

In the past and nowadays usually only energetic issues related to renewability or un-renewability have been analyzed. But the most critical point of the non-renewable sources is that they are geographically concentrated only in some areas. On the other hand, renewable sources minimize the issues related to the time (no depletion risk) and also reduce the issues related to the space as they are usually homogeneously geographically distributed, but in order to really taking advantage from renewables, storage techniques have to been designed.

Usually the energetic issues are contextualized as economic issues, implicitly considering all mankind as an homogeneous entity. What really happens is that some people can hoard energy as much as they need while other people have to live with extremely poor energy supplies: the inequality is the rule and not the exception! [4]. This means that energy issue is in small part an economic issue and in large part an ethical issue. Increase the renewable sources utilization and develop new energy storage strategies means to reduce the inequality of the mankind.

As said at the beginning, energy is related to every activity and all people's needs are conditioned by it. As an example, common cereals price trend follows pretty well the oil price trend. This happens because now days oil is the world main energy source and its price influences also the price of other energy sources. But if the

2

food price increases, a large part of the world population gets into trouble and this is another confirmation of the relation between energy and nation's power.

The real viable solution, combined with the renewable sources, consists in the energy saving. Once the energy supply is fixed or limited both by physiological and geopolitical constraints, people have to work on the energy demand side. Every MWh of avoided consumption has the same impact of a MWh additional produced. From the standpoint of nations independence and emancipation, governments should work more on energy saving respect to the increase of energy production.

Periodically, nuclear source is assumed as the definitive solution of all energy issues. Considering present technology (fission reactors) and, as an extreme hypothesis, assuming negligible safety issues, nuclear energy is definitively a non-solution to the energetic problem. The reason is that it maximizes the geolocation issues because feedstocks are concentrated in certain areas only and the zones where slags are stored are hugely penalized [5].

Concluding, it is very interesting to compare the map of the wars and inequalities respect to the map of the energy sources [6] [7]. This aspect deserves a dedicated depth analysis that unfortunately can't be here addressed.

Energy storage: the key of the energetic revolution

Renewable sources are assumed as a big contribution for the solution of the energy problem. As a consequence the renewable sources emphasize the need of the energy storage. As briefly said before the two most important leverages in world government are the energy and the ability to issue (and well manage) money. As a consequence economic aspects can have strong influences on some energetic scenarios and vice versa. Specific energetic policies can directly or indirectly influence renewable and storage technologies. As an example, energy grid imbalances, caused by intrinsic characteristics of the renewables and by difficulties in prediction of users energy demand, are nowadays penalized by additional fees. This yields an improvement in researches concerning smart cities and smart grids and more attentions in researches in storage capabilities of the existing power plants. Some economic policies can promote certain scenarios and

solutions even if they are characterized by poor efficiency. This implies that storage solutions can be evaluated not only from an efficiency standpoint but also considering overall economic aspects.

Life quality, inequality reduction and independence of nations are aspects that are usually not considered when high level policies are determined. In the rest of the thesis, present technologies and new devices design are evaluated in terms of costs and efficiency. Nevertheless the right standpoint in order to evaluate a storage solution is to consider what kind of improvements can bring in all mankind and how big are the impacts on primary resources. In this sense storage of renewables sources is always a profitable solution. The real cost that has to be calculated is the one concerning the materials of the storage devices. If the ecological balance is reached for a particular storage solution, it certainly can be used and all other constraints (usually economic constraints...) are fictitious and are imposed only because the energetic problem is observed from the wrong point of view.

[1] V. Smil, Energy In World History (Essays in World History), Westview Press, 1994.

[2] G. Barker, The Agricultural Revolution in Prehistory: Why did Foragers become Farmers?, Oxford University Press, 2009.

[3] P. Barnard, Il più grande crimine, Edizioni Andromeda, 2011.

[4] «The World Top Incomes Database,» [Online]. Available: http://topincomes.g-mond.parisschoolofeconomics.eu/.

[5] I. A. E. Agency, «World Distribution of Uranium Deposits (UDEPO) with Uranium Deposit Classification,» IAEA, 2009.

[6] «World Energy Council,» [Online]. Available: http://www.worldenergy.org/.

[7] «Wars in the World,» [Online]. Available: http://www.warsintheworld.com.

Chapter 2
Solid oxide Electrolysis Cells (SOEC)

Outline

In this chapter the reader will be introduced on Solid Oxide Cell (SOC) physic and technology in general with particular details concerning Solid Oxide Electrolysis Cell (SOEC).

At the beginning thermodynamic basis are presented and some general relations are shown. The aim of this part is to emphasize the multi-physic nature of the SOEC devices and to derive some general constraints that will guide the modeling approach and stack design described in the next chapters.

Then a brief overview of past and present SOEC devices configurations is reported. In this paragraphs the description of the evolution of stack architectures is presented taking into account the general framework that has influenced the devices design. In addition some details are provided in order to purpose SOEC devices as chemicals devices and not energy devices.

As the physic and the technology are described some SOEC chains are proposed in order to evaluate viable future scenarios. Different approaches are considered and a single global efficiency parameter has been derived in order to compare them. For those chains that are far from economic constraints some prescriptions or key concepts are provided to emphasize the weaknesses and the bottleneck of the scenario.

High Temperature Electrolysis (HTE)

The thermodynamic bases of high temperature electrolysis can be found in (1). For pure hydrogen and oxygen streams, from an overall chemical reaction standpoint, the water splitting process corresponds to the dissociation of water

$$H_2O \rightarrow H_2 + \frac{1}{2}O_2, \qquad \Delta H^0_{298K} = 285.84 \ kJ/mol$$

while for co-electrolysis the carbon dioxide splitting process, considering the leading reaction only, corresponds to

$$CO_2 + H_2 \rightarrow CO + H_2O, \qquad \Delta H^0_{298K} = 41 \ kJ/mol$$
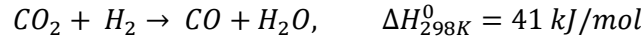
The net enthalpy increase of the reaction products over the reactants is defined as

$$\Delta H_R = Q - W$$

Where Q is the heat exchanged and W is the external work. For reversible operation it can be derived

$$W_{rev} = \Delta H_R - T\Delta S_R = \Delta G_R$$
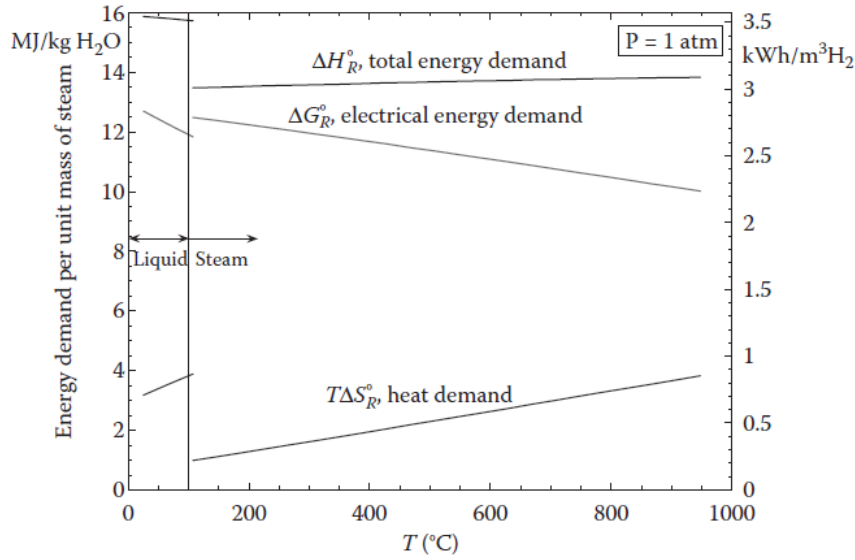
Figure 1: Standard-state ideal energy requirements for electrolysis as a function of temperature (1).

Figure 1 shows that for reversible reacting system operation the electrical work requirement (the Gibbs free energy change ΔG_R) decreases with increasing temperature, while the term $T\Delta S_R$ increases. Note that the total energy requirement (ΔH_R) increases only slightly with temperature.

In order to accomplish electrolysis, a voltage must be applied across the cell that is greater magnitude than the open-cell potential given by:

$$V^0 = \frac{\Delta G^0_R}{jF}$$

where j is the number of electrons transferred per molecule of hydrogen produced (j is equal to 2 for the steam-hydrogen system). In practical cases open circuit voltage is affected by real operating conditions that consist in diluted reactants feedstock especially at oxygen side where usually air is provided reducing the oxygen partial pressure to only about 21% of the operating pressure.

Solid oxide electrolysis operating mode is fundamentally different than fuel cell operating mode. This is mainly due to the standpoint of heat transfer. In fact SOFC operationg mode usually requires significant excess air flow in order to cool down the stack. The overheating is due both to the exothermic nature of the hydrogen oxidation reaction and to loss heating related to ohmic ionic resistance and electrodes activation. On the other hand in the electrolysis mode the steam reduction reaction is endothermic. Therefore, depending on the operating voltage, the net heat generation in the stack may be negative, zero, or positive as depicted in Figure 2.

The ohmic heat flux has always an exothermic contribution and is given by

$$q_{Ohm} = i^2 ASR$$

where i is the current density and ASR is the area specific resistance. The reaction heat flux is given by

$$q_{Ohm} = \frac{i}{2F} T\Delta S_e$$

where ΔS_e is the entropy change for the process and change is sign between electrolysis and fuel cell operation mode. This implies that In the fuel cell operating mode the net heat flux is always positive and increases rapidly with operating voltage. In the electrolysis operating mode the net heat flux is negative for low operating voltages, increases to zero at the thermal-neutral voltage, and is positive at higher voltages and current densities. Following passages reported in (1). the thermal-neutral voltage can be predicted as

$$V_{tn} = \frac{\Delta H_R}{2F}$$
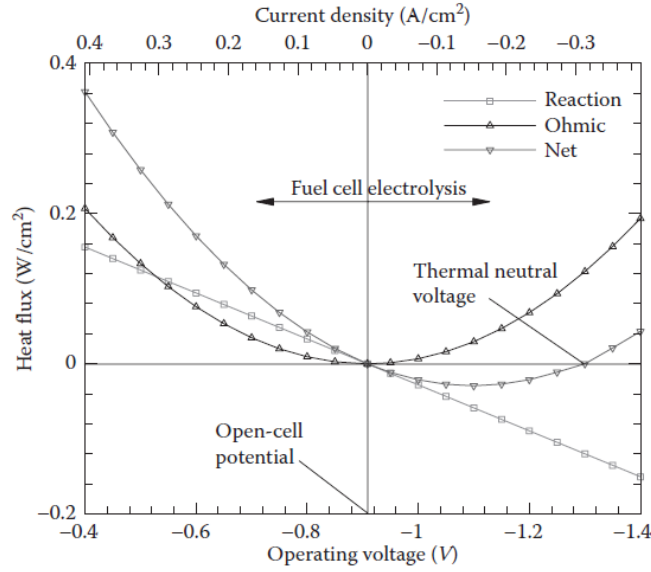
Figure 2: Thermal contributions in electrolysis and fuel cell modes of operation (1).

For typical SOEC cells, thermal-neutral voltage yields medium-high current densities (greater than 0.5 A/cm2) and the better are the cells performances (low ASR) the higher is the thermal-neutral voltage (and related current density). Operation at temperature equal or greater that thermal-neutral voltage simplifies thermal management of the device because no additional heat has to be provided especially considering that such heat has to be provided at very high temperature. Furthermore in order to design the stack as a reversible device slight exothermic operating condition is preferable in order to obtain similar thermal condition both for SOFC and SOEC operating mode.

The electrolysis efficiency η_e can be defined for HTE, analogous to the definition of fuel cell efficiency

$$\eta_e = \frac{V_{tn}}{V_{op}}$$

that yields values of the efficiency greater than 1.0 for operating voltages lower than thermal neutral.

SOEC devices

The solid oxide cells are a solid-state electrochemical devices consisting of an oxygen-ion-conducting electrolyte with porous electrically conducting electrodes placed on either side of the electrolyte.

The standard electrolyte material is zirconia doped with yttria is called yttria-stabilized (YSZ) that is a good oxygen ion conductor. In the electrolyte holes in the oxygen sublattice are introduced and it makes possible for oxygen ions to move through the solid. The most common steam and hydrogen electrode (cathode in electrolysis mode) material is porous nickel-zirconia (YSZ) cermet. A nickel-ceria cermet can also be used. Because the cathode contains nickel metal, reducing conditions must be maintained on this electrode during cell operation. The nickel in the cathode acts as an electronic conductor and as a catalyst for steam reduction. The zirconia in the cermet provides ionic conductivity. The electrochemical reactions to the triple-phase boundary (TPB) where the electronic, ionic, and gas phases coexist. Several materials have been studied for the oxygen electrode (anode in electrolysis mode) that operates in a highly oxidizing environment. The most common material used is strontiumdoped lanthanum manganite, La0.8Sr0.2MnO3, or LSM (perovskite material) that material provides good electronic conductivity and good catalytic activity.

Several cell and stack designs have been developed both for SOFC and SOEC applications. The cell design highly influences the stack design. Solid oxide cells can be electrode supported (steam electrode or oxygen electrode), electrolyte supported or metal supported. Concerning the cell shapes two main configurations have been proposed in the past years: the planar configuration and the tubular configuration. Planar design provide in general better performances and higher power density. Contrary tubular configuration shows more robustness and durability especially concerning the complete stack (1). Both designs are based on separated gas chambers, one for the oxygen or air and the second one for steam and hydrocarbons. The electrodes and electrolyte conduct electrical current through the cell and electrons can direct to the external current takes directly through metal separator plates or through conductive foams and meshes.

The electrochemical half-cell reactions are the steam electrochemical reduction

$$H_2O + 2\,e^- \rightarrow H_2 + O^{2-}$$
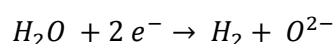
and the oxygen synthesis

$$O^{2-} \rightarrow 2\,e^- + \frac{1}{2}O_2$$
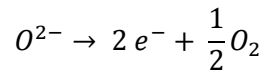
In electrolysis mode the electrons flow from the anode to the cathode by means of an external power source. The electrolyte conducts the charge carriers from the cathode to the anode. Oxygen ions are drawn through the electrolyte by an applied electrochemical potential. The ions liberate their electrons and recombine to form molecular O_2 on the anode side.

SOEC chains

SOEC devices can be used as a key device in some energy chains (2) (3) (4) (5) (6) (7). As will be shown later on from an efficiency and economic point of view mostly of them are not viable. But if strategic or geo-politic issues are also considered all chains can be evaluated profitably.

Power to gas: methane production with co-electrolysis

This chain consists in a co-electrolysis SOEC stack feed by steam, carbon dioxide and renewable energy in order to produce methane. SOEC products are carbon monoxide and hydrogen and methane synthesis can take place both directly inside the SOEC device and (the major part) in a dedicated reactor. Using separate reactor it is possible to extend the Fischer-Tropsch reactions (8) in order to obtain heavier fuels. Figure 3 schematically shows the chain.
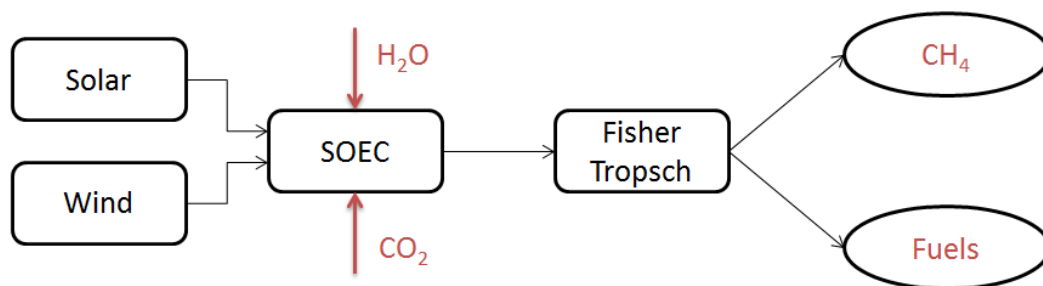

Figure 3: SOEC power to gas chain: methane production with co-electrolysis

The chain efficiency is calculate as the ratio between the amount of energy that can be directly provided to the grid with the energy that can be delivered in other form depending by the considered chain. In order to make more clear the comparison for chains that provide energy in chemical form also an economic index is calculated. Reasonable efficiency value both for SOEC devices and Fischer-Tropsch reactors are $\varepsilon = 90\%$ that yield an overall efficiency near to $\varepsilon_T = 80\%$. This value can be little higher if the considered renewable energy comes from solar source (alternator is not required) and can be little lower if the considered renewable energy comes wind (rectifier has to be considered). The overall energy efficiency is quite appreciable, but the economic index shows worst performance. In fact the economic exploitation of the electrical energy considering the present Italian market is about $40 – 50$ €/MWh, while the methane economic exploitation is around $20 – 30$ €/MWh. This means that the economic index is equal to $40\% – 50\%$. Furthermore the co-electrolysis device has intrinsic complexities do to the cell degradation respect to the steam only electrolysis that increase the global costs (capital and maintenance costs) of the devices. As shown later on this chain is less convenient respect to similar ones. The advantage in Fischer-Tropsch reactors is the possibility to synthetize more complex hydrocarbons and obtain liquid fuels characterized by high purity.

Power to gas: methane production with steam electrolysis only and successive separated methane synthesis

This chain is conceptually similar to the previous one. High temperature electrolysis is performed with steam only and the carbon dioxide is provided downstream is a separated Sabatier reactor (9). Chain scheme is shown in Figure 4. Assuming the efficiency of the Sabatier reactor similar to the Fischer-Tropsch reactor the overall chain efficiency is equal to the previous one. Same considerations concerning the economic index. The only difference between the two chains consist in the capital and maintenance cost of the devices. In fact steam electrolysis is simpler that co-electrolysis and cells durability is considerably higher. This means that if power to gas chains, considering economic and strategic analysis, are considered viable the high temperature steam electrolysis combined with Sabatier reactor will be the optimal choice.
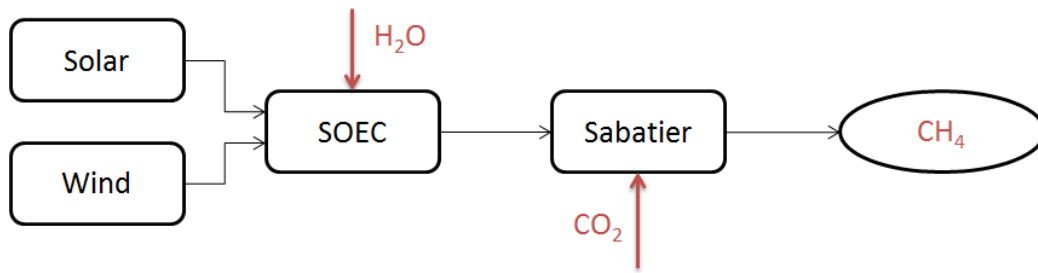
Figure 4: SOEC power to gas chain: methane production with steam electrolysis only and successive separated methane synthesis

Power to gas: hydrogen production

In this scenario the output of the chain is directly the hydrogen. The SOEC perform steam electrolysis only with the advantages previously discussed. Even if the hydrogen can be stored (experimentally) and used as primary fuel the only viable solution consists in directly supply the existing methane grid. Limitations have to been considered depending to the grids. This implies that massive hydrogen production can't be taken into account. Figure 5 schematically shows the chain.
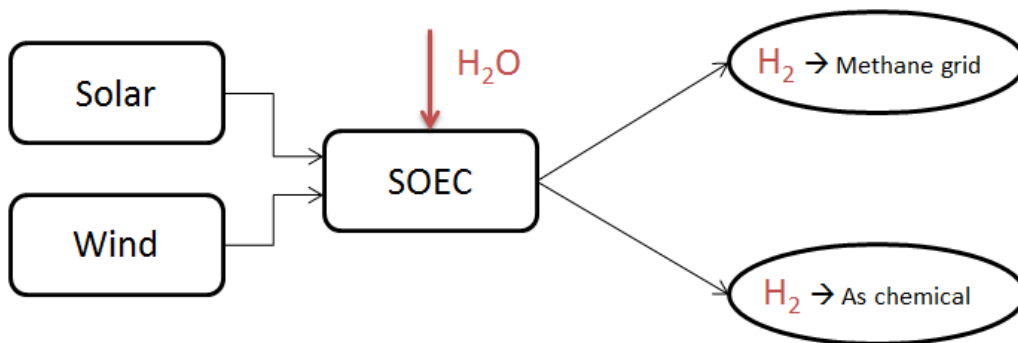

Figure 5: SOEC power to gas chain: hydrogen production

Considering the efficiency the main losses are due to the SOEC devices. Thus an overall efficiency equal to 90% can be considered. From an economic standpoint now days there isn't a real hydrogen market concerning hydrogen utilization as a fuel. Considering that the hydrogen in the methane grid has the effect to increase the heating value reducing the volumetric consumption it seems reasonable to assuming for the hydrogen the same economic exploitation of the methane. This implies that an

Power to power

The weakness of the previous solutions is the low economic exploitation of the produced fuel. An SOC device can operate in reversible mode in order to provide a power to power chain. The first advantage of this scenario concerns the higher economic exploitation of the chain output. The second advantage consists in the flexibility of the chain providing the capability to work in storage mode when energy price is low and to work in production mode when energy price increase both following short (daily) and medium period variations.

Co-electrolysis can be considered as described before in order to obtain methane to be stored. Storage of hydrogen or carbon monoxide mixtures can be taken into account both for economic reasons and for safety issues. Thus in case of steam electrolysis a Sabatier reactor has to be considered in order to obtain methane.

Energy production is obtained with the same SOC device operating in fuel cell mode. This implies that even if SOC cell can be operate in a steam only environment during the storage, carbon related issues have to be taken into account during the energy production. Chain scheme is shown in Figure 6.
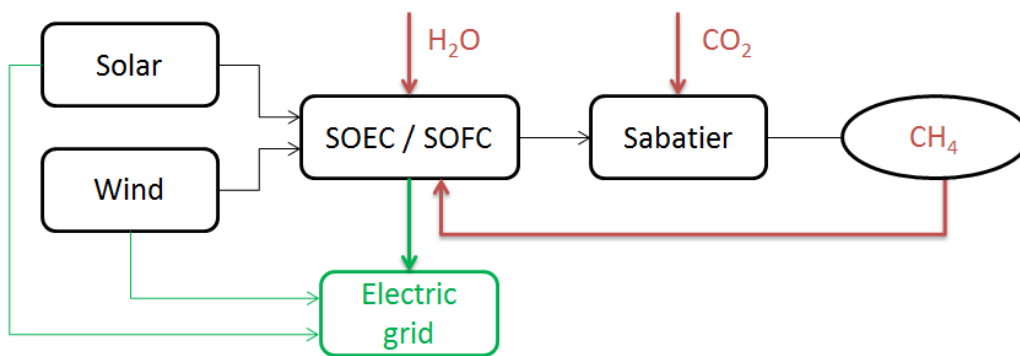

Figure 6: SOEC power to power chain

The overall efficiency is obtained combining the efficiency of the storage ($\approx$80%) with the efficiency of the SOFC operation mode ($\approx$60%) that yields an overall value about 50%. From an economic standpoint this chain has the same performances of the previous ones. The big advantages of this chain consists in the leverage that can be applied managing and shifting the storage phase respect to the production phase that in some scenarios can considerably increase the economic exploitation of the output energy.

Power to chemicals

The last chain presented is related to a non-storage approach. As shown in the previous paragraphs the main limitation is that appears more convenient to produce energy in more clever way respect to store it and this penalize the energy storage chains. In order to maximize the economic output of the SOEC devices it has to be considered that the products of the co-electrolysis are the main bricks of the very high value green chemicals. This can represent the killer application of the technology and even if is not trivial to generally evaluate advantages and criticisms this chain has to be considered in order to increase the diffusion of the SOEC devices. In fact as shown in Figure 7 chemicals are very profitable and can minimize the impact of the SOEC devices capital costs especialy during the technology early stages.
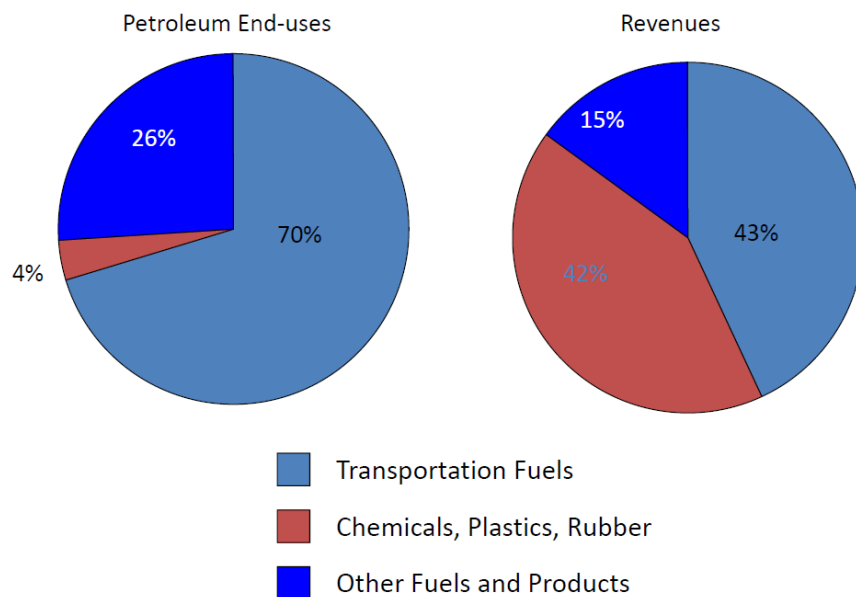

Figure 7: Petroleum incomes (10)

Conclusions

In this chapter an overview of the SOEC devices has been provided. Thermodynamic fundamentals are been shown in order to identify the most important parameters that have to be taken into account in SOEC stack design. Temeprature has been identify as the key parameters concerning efficiency and has to be maximize compatibly with technological constrainst.

Even if efficiency is very important in the market diffusion of the SOEC, the real bottleneck of the technology, consisting in the decreased economic exploitations of the SOEC output, has been individuated perfomring different chains evaluation. This analysis leads to two high value chain: the power to power chain considering controllable shifting between storage and production phases and the power to chemical chain.

1. *Nuclear Idrogen Production.* s.l. : Yan, X., L., Hino, R., 2011.

2. *Sustainable hydrocarbon fuels by recycling CO2 and H2O with renewable or nuclear energy.* **Graves, Christopher, et al., et al.** 1, 2011, Renewable and Sustainable Energy Reviews, Vol. 15, p. 1-23. ISSN: 1364-0321 DOI: http://dx.doi.org/10.1016/j.rser.2010.07.014.

3. *Recent advances in high temperature electrolysis using solid oxide fuel cells: A review .* **Laguna-Bercero, M.A.** 0, 2012, Journal of Power Sources , Vol. 203, p. 4-16. ISSN: 0378-7753 DOI: http://dx.doi.org/10.1016/j.jpowsour.2011.12.019.

4. *The feasibility of synthetic fuels in renewable energy systems.* **Ridjan I., Vad Mathiesen B., Connolly D., Duić N.** 1 August 2013, Energy, Vol. 57, p. 76-84. 0360-5442.

5. *Hydrogen and synthetic fuel production using high temperature solid oxide electrolysis cells (SOECs).* **Kazempoor P., Braun R.J.** 9, 9 March 2015, International Journal of Hydrogen Energy, Vol. 40, p. 3599-3612. 0360-3199.

6. *Electrochemical devices for energy: fuel cells and electrolytic cells.* **Cassir M., Jones D. ,Ringuedé A., Lair V.** 2013, Handbook of Membrane Reactors, Vol. 2, p. 553-606. 9780857094155.

7. *Power to gas: Technological overview, systems analysis and economic assessment for a case study in Germany.* **Schiebahn S., Grube T., Robinius M., Tietze V., Kumar B., Stolten D.** 12, 6 April 2015, International Journal of Hydrogen Energy, Vol. 40, p. 4285-4294. 0360-3199.

8. *Production of Fischer Tropsch liquid fuels from high temperature solid oxide co-electrolysis units.* **Becker, W.L., et al., et al.** 1, 2012, Energy, Vol. 47, p. 99-115. Asia-Pacific Forum on Renewable Energy 2011 . ISSN: 0360-5442 DOI: http://dx.doi.org/10.1016/j.energy.2012.08.047.

9. *Parametric study of an efficient renewable power-to-substitute-natural-gas process including high-temperature steam electrolysis.* **De Saint Jean M., Baurens P., Bouallou C.** 13 October 2014, International Journal of Hydrogen Energy, Vol. 39, p. 17024-17039 ISSN. 0360-3199.

10. **T., Werpy.** BIO-World conference in Biotechnology and Bioprocessing. Montreal : s.n., 19-22 July 2009.

Chapter 3
SOC modeling techniques

Outline

In this chapter some approaches and techniques concerning SOC modeling are presented. First the global modeling philosophy and main issues and limitations are reported. The reader is then introduced in the general modeling framework starting from physical and numerical models definition, proceeding in the approximations definition process and finishing with the simulations set up.

In the present work two approaches have been used concerning the numerical approaches: the Finite Volume Method (FVM) for computational fluid dynamic (CFD) and Finite Element Method (FEM) for thermal and structural analysis. For FEM analysis commercial codes have been used using their standard implementation. For CFD analysis a complete SOC solver has been developed from scratch basing on the open source OpenFOAM® tool. The code uses the robust steady state and transient pressure-velocity coupling algorithms already implemented in the main OpenFOAM release and presents innovative routines concerning multispecies diffusion and SOC peculiar domains handling. The solver can predict both the polarization curves and the impedance spectra curves as described later on. Additional details concerning this code are reported in the next paragraphs.

As already said one of the main characteristic of the SOC in-house developed code is the capability to predict the overall SOC performance in term of current density and voltage. Typical models set up for this specific purposes are characterized by two fluid domains (fuel side and oxygen side) each of them coupled with a porous domain (the electrodes). The SOC interface is set between this two domains. All fluid conditions are set at the boundary in order to be numerical consistent. Both total current and voltage can be used in order to define the operating point. Thermal data (temperature and thermal fluxes) can be exchanged either with a solid domain implemented in the CFD solver (two-way coupling) or with other dedicated external tools (one-way coupling). Both steady state and transient simulations can be run and reduced numerical domains (i.e. only the fluid domain in order to quickly analyze some aspects assuming the air

domain as "frozen") can be handled. The common outputs of this kind of simulations are the current-voltage polarization, the thermal field distribution and the fluid and species field distributions (velocity, pressure, concentrations, etc…).

The second main characteristic of the code is the capability to handing the SOC impedance spectra. Typical models set up for this specific purposes are very similar to the ones set up for the polarization with the exception that they are transient only and accept sinusoidal total current or voltage as input. Simulations start from a defined operating point previously calculated and compute the perturbed status generated by the oscillating input data. The solver run the simulation for a user defined number of periods and then shift to an higher frequency. Due to computational reasons usually the thermal field external respect to the fluid domain is assumed to be "frozen". The common outputs of this kind of simulations are the impedance spectra calculated basing on the input voltage/current and the output current/voltage and the characteristics derived quantity (i.e. high frequency intercept, low frequency intercept, etc…). The spectra can be calculated for different operating points also.

At the end of the chapter the reader should be aware of the potentialities, the issues and the limitations of the SOC numerical modeling capability. In addition some choices and modeling assumptions presented in the next chapter dedicated to the design an innovative SOEC are then justifiable.

Modeling background

One of the main aspect that has to be stressed in modelling is the difference between simulation and emulation. The term simulation means "to reproduce the causes", while on the other hand emulation means "to reproduce the effects". By definition, in a multi-scale approach phenomena simulated in an high detailed low-level model are then emulated in the top level model, and often the link between the two scales is not trivial (1). This is due because in simulation a large space of parameters can be studied well reproducing the effects, while in emulation this is not always true. One can imagine the emulation as a sort of multi variable linearization. In complex models, after defining a base time and space scales as the reference ones, parts of the model are based on real simulation, while other parts are based on emulation due to practical physical or

computational issues. This theoretical approach has to be taken into account during the interpretation of the model results. Sometimes one can get into errors when increasing the level of detail of the simulated aspects, forgetting to properly handling the emulated ones.

Often, emulation is need not only for computational limitations but also due to evaluation of uncertain parameters. Usually, low scale models are characterized by huge number of parameters, which most of the cases are determined in ideal conditions. The interdependency of that parameters increases the complexity of the model and also increases the degrees of freedom: in fact, in practice some of these parameters are used as tuning parameters. In that case, the risk to obtain a very good detailed model characterized by an high number of "free" parameters is absolutely present (2) (3). This means that this kind of model can well reproduce the experimental results but characterized by very bad robustness. In fact, if a Monte Carlo simulation is performed on that models considering the space variability of all these parameters, simulations results with extremely big error bars can be obtained. Hence, in that case an emulation approach is preferable because in this way it is possible to considerably reduce the number of parameters and better interpret Monte Carlo analysis. Furthermore it is possible to reach a higher awareness of the limitations of the model that is a mandatory aspects for whom uses modeling in general.

Finally, to help the reader in the rest of the thesis, the difference between the terms homogeneous and uniform is reminded: "uniform" means that a variable or a parameter doesn't change its own value during the time, while "homogeneous" means that a variable or a parameter doesn't change its own value in space. These concepts are very useful during transient simulations as numerical/physical quantities can vary both in space and in time.

SOC devices are essentially described by two-chambers reacting systems where some gases enter in and many homogeneous and heterogeneous reactions take play (4). The two sub systems are linked through some electrochemical reactions influenced by the external applied load. The physical domains usually involved vary from solid domains (i.e. the metallic interconnector part or the insulating), to low-porosity porous domains (i.e. the electrodes), to high-porosity porous domain (i.e. the compressed insulating layers or the solid electrolyte). Multi species diffusion has to be considered for gaseous species and usually laminar conditions are assumed. Leading gases react with their self and many radicals and secondary species are then generated. These species catalytically react with solid species and form other derived compounds and

mixtures. A complete physical model has to take into account homogeneous reaction inside gas diffuser, heterogeneous reactions inside electrodes pores and with metal surfaces (both coupled with the effects generated by the applied voltage or total current), electrochemical reactions at Three Phase Boundary (TPB) proximity and solid diffusion inside solid elements. In addition phases changes, evaporations and adsorption/desorption have to be considered to predict the real device behaviour. The only way to take into account all this phenomena is to model the system at very low time and scales level. The order of magnitude of the space scale is 10^{-9} m. This means that no cell-level or stack-level models that consider all this aspects can be realistically calculable.

The equations and relations involved in a complete model are usually very complex and computational expensive but this is not the main limit for such kind of models as usually believed. In fact the common approach is to simplified the relations and equations (considered too computational demanding), then independently chose the space scale and consequentially the time scale. Contrary the right approach that has to be considered is to first select the space scale (as low scales are not calculable for the complete domain), then neglect phenomena that take place at low space scales and finally adapt the time scale. Figure 1 shows a schematic representation of this concept.

Low scales phenomena can be taken into account, but only through relations and approximations derived from other models and at high level models it is only possible to study the effects of these assumptions/relations and not to study these phenomena their self. Even if this considerations seem to be obvious they are often neglected. As an example of this concepts one can consider that at stack level is possible to show the effects of a particular predefined degradation model but is not possible to study the degradation model itself.
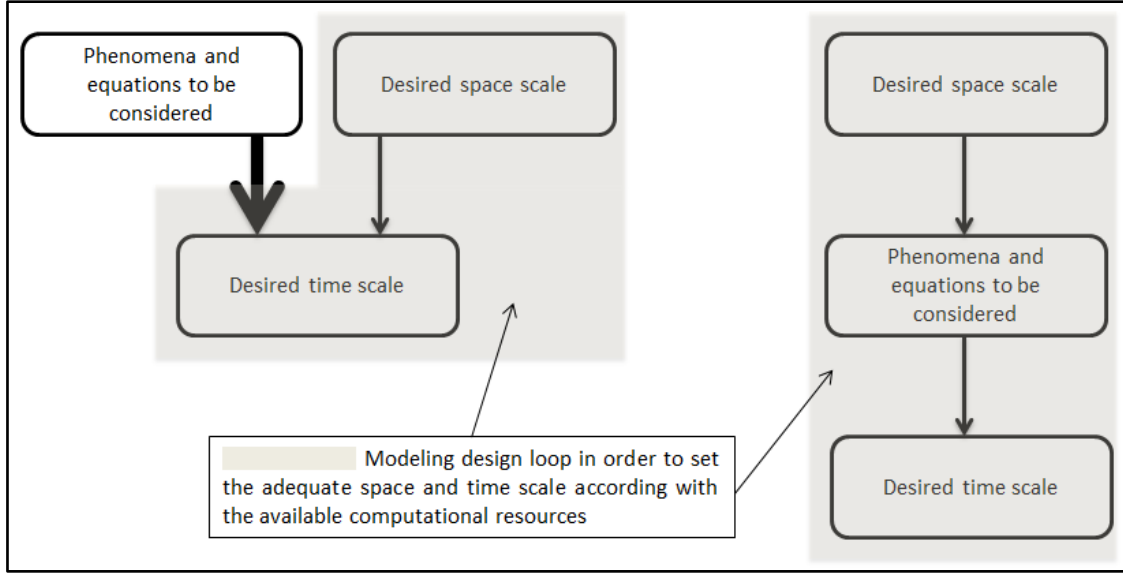
Figure 1: Schematic representation of common modeling desing (sx) and righ modeling desing (dx)

Mathematical modeling

In order to describe the physic of SOC stack the limit of the laminar flow where density variations and are not correlated with pressure variations (low Mach number) is consider (5). For gases mass and momentum conservation the well-known multispecies compressible Navier-Stokes equations in the low Mach number approximation are considered. The continuity equations set for a gas with non-constant density is:

$$\frac{\partial \rho_\alpha}{\partial t} + \nabla \cdot (\rho \overrightarrow{v_\alpha}) = \mathbf{S_{y_\alpha}} \tag{3.1}$$

where ρ_α is the gas partial density, ρ is the density of the mixture, $\overrightarrow{v_\alpha}$ is the species velocity and $\mathbf{S_{y_\alpha}}$ is the species mass source. Using single-fluid multispecies approximation, conservation equations for species assumes the form

$$\frac{\partial \rho y_\alpha}{\partial t} + \nabla \cdot (\rho y_\alpha \vec{v}) + \nabla \cdot \overrightarrow{J_\alpha} = S_{y_\alpha} \tag{3.2}$$

where y_α is the gas mass fraction, $\vec{v}$ is the mixture mass average velocity and $\overrightarrow{J_\alpha}$ is the species diffusive mass flux. In porous media the mass average velocity $\vec{v}$ is substituted by the permeation velocity $\overrightarrow{\langle v \rangle}$ and the temporal derivative is damped by the porosity ε.

The momentum equation for the mean flow is defined by

$$\frac{\partial \rho \vec{v}}{\partial t} + \nabla \cdot (\rho \vec{v} \vec{v}) - \nabla \cdot \vec{\vec{\tau}} = -\nabla p \tag{3.3}$$

Where $\vec{\vec{\tau}}$ is the viscous stress tensor and p is the pressure. In the case of porous media, again porosity damps the momentum equation components, and porous permeability and porous inertia tensor play a specific role. A complete review of these equations applied on solid oxide cells is presented in (6). Using single-fluid approach it is easy to consider other external force (gravity, centripetal acceleration, etc..) in equation 3.3. Electric and magnetic driving forces usually act only on charged species and in SOC modeling their effects are supposed to be negligible in momentum equation.

In equations 3.2 diffusive mass fluxes are present. These fluxes can be modeled in different way and with different approximation level. Models vary form the simplest Fick model, even with correction for porous media (Bousanquet model) to more complex models such as Maxwell-Stefan model for multispecies system and dusty gas model (7) for electrodes porous media. All these models contain binary diffusion coefficients and for that coefficients in literature many sub-models have been developed, i.e. Chapman-Enskog, Wilke-Lee, Fuller-Schettler-Giddings. From the kinetic gas theory Knudsen corrections are also proposed (6). Most of them are temperature and/or pressure dependent, that implies a more complicated dynamic response for the global system.

The energy equations for multispecies flow is:

$$\frac{\partial \rho h_s}{\partial t} + \nabla \cdot (\rho h_s \vec{v}) - \nabla \cdot (\alpha \nabla h_s) + \nabla \cdot \left[\alpha \sum_{i=1}^{N} \left(h_{s_i} \nabla y_i \right) \right] + \nabla \cdot \left[\sum_{i=1}^{N} \left(\vec{j_i} h_{s_i} \right) \right] = S_i \tag{3.4}$$

where h_s is the mixture sensible enthalpy, h_{s_i} are the species sensible enthalpies, α is the thermal diffusivity and S_i is the heat source.

SOC solver: general description

The in-house developed SOC solver is based on OpenFOAM® framework. The code is compatible both with the official release (2.3.1) distributed by ESI and the community-driven release (foam-extend-3.1). Additional information concerning the OpenFOAM® releases can be found in (8) and (9).

The solver solves the equation set 3.3 using the standard routines implemented in the main tool. In addition the species equation set 3.2 has been upgraded and linked with a multispecies diffusion library in order to handling different diffusion models. Concerning the mean flow some corrections are implemented in the energy equation 3.4 in order to make consistent all the equation set. In particular the two last terms on the left end side of the equation 3.4 has been introduced as they are not considered in the standard OpenFOAM® formulation. The implementation of the boundary condition for species field has been improved in order to take into account all the update done to the main code.

The electrolyte interface has been completely developed from scratch. The interface is supposed to have uniform voltage distribution and for each computational cell of the domain a local value of the Nernst potential has been defined. The Nernst equation links the species partial pressures and the temperature to the potential difference across the electrolyte. SOC performances are fundamentally described by this equation that essentially define "how big" is the driving force acting on charge carriers.

$$E = E^0 + \frac{R\,T}{2\,F}\ln\left(\frac{p_{H_2}\,p_{O_2}^{1/2}}{p_{H_2O}}\right) \tag{3.5}$$

As an example, equation 3.5 represents the Nernst equation for an electrochemical system with hydrogen, water, oxygen and other inert gases, where E is the Nernst potential, E^0 is the potential at reference state, R is the gas constant, F is the Faraday constant, T is the absolute temperature and p_α are the gas partial pressures. In this work second order dynamic effects of the oxygen ions mobility, well considered in the Poisson-Nernst-Planck equation, are assumed to be negligible. For other electrochemical systems different value of E^0 can be defined usually basing on correlation function of the working temperature and the functional dependency respect to the partial pressures depends on the specific electrochemical system. Equation 3.5 also shows that local variation of partial pressures and temperature dynamically influences the Nernst potential.

In the electrolyte subroutine of the OpenFOAM solver the relations between current density and species consumption/production are implemented. For all computational cells in the electrolyte domain local current density is calculated considering different contributions (ohmic losses, activation losses, etc...). There are no limitations in term of potential drop models. Common implementation consist in two contributions (fuel side and air side) based on Buttler-Volmer equation and one or more additional linear contributions for taking

into account the ohimc losses. For the transient simulations to compute the impedance spectra, voltage drop elements with particular dynamic behavior are also implemented as described later on.

If the external load is applied by providing the voltage value the general non-linear loop in each cell is repeated adapting the local current density until the imposed voltage value is reached. If the external load is applied by providing the total current an additional external numerical loop is implemented in order to tune the voltage that give the prescribed total current value. The first solver operating mode (assigned voltage) is more efficient because one numerical loop is avoided while the second solver operating mode (assigned total current) has the advantage that it is more compliant with the experimental approach. In both cases the current density shape function (the distribution along the electrolyte) is obtained as a solver output.

As the local current density is known the electrolyte routine computes species molar and mass fluxes and update the boundary conditions in a consistent way in order to guarantee the continuity.

SOC solver: polarization and flow field modeling

In this work many numerical simulations are set up in order to reproduce the experimental results and in order to predict physical behaviors. For each simulation the implemented boundary condition are summarized in Table 1.

	Inlets	Outlets	Electrolyte interface	Other boundaries
Species mass fractions	Fixed fluxes (Fixed value)	Zero diffusive flux (Zero gradient)	Fixed flux (Faraday equation)	Zero flux
Mass average velocity	Fixed value (Fixed flux)	Zero gradient	Non sip condition	Non sip condition
Pressure	Zero gradient	Fixed Value	Zero gradient	Zero gradient
Temperature	Fixed value	Zero diffusive flux (Zero gradient)	Fixed flux	Adiabatic or external heat exchange

Table 1: Common boundary conditions for transient and steady state SOC modeling

The solver intrinsically works in both operating modes (SOFC and SOEC) and the user can switch between them only assigning positive (SOFC) or negative (SOEC) total current value or assigning a voltage value

lower or greater the theoretical Nernst one. If small perturbations are applied near the Open Circuit Voltage (OCV) the solver can compute the non-trivial equilibrium solution that consist in a slightly non uniform current density and species field distribution. This simulations can show the little recirculating current typical of the OCV conditions.

Figure 2: SOFC/SOEC polarization (a) and table with the main operating conditions (b)Figure 2 shows the input data and the results of a simulation performed on a circular cell in a unsealed set up. In the specific in this simulation the reactant utilization not exceed the 50% and this is why the electrolysis polarization looks very similar to the fuel cell polarization.

Data type	Value
Inlet condition (molar fractions)	$H_2 = 20\%$
	$H_2O = 80\%$
	$O_2 = 21\%$
	$N_2 = 79\%$
Geometry description	Circular cell not sealed
Temperature	800 °C
Operation mode	SOEC/SOFC

(a)

(b)
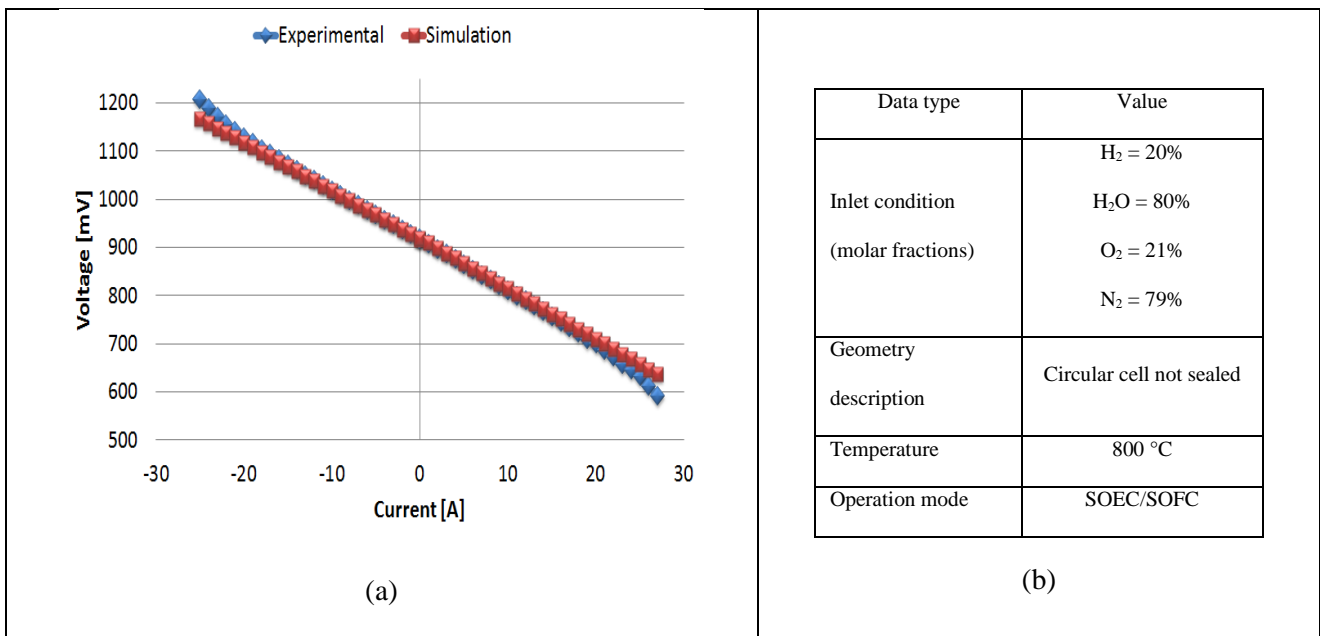
Figure 2: SOFC/SOEC polarization (a) and table with the main operating conditions (b)

In Figure 3 some other results obtained with the in-house developed solver are presented. In this figure (Figure 3 – b) is evident the non-linearity of the species concentration that considerably penalize the ending part of the cell. This can be showed more clearly in Figure 3 – c where high reactant utilization is reached. In this case the current density shape function is quite uniform in the central part of the cell and dramatically drop toward the end. The ending area of the cell presents very low current density near the zero value. In this region adjacent cell region operate in inverse condition (from fuel cell from to electrolysis operation conditions) and they don't give a contribution to the total current density. The greater is the applied voltage drop the more the zero-current area increase and the more is the current density in the inner region of the

cell. This high non-uniformity involve thermal aspect also with harmful effects on cell performance and in cell Mean Time Between Failure (MTBF).
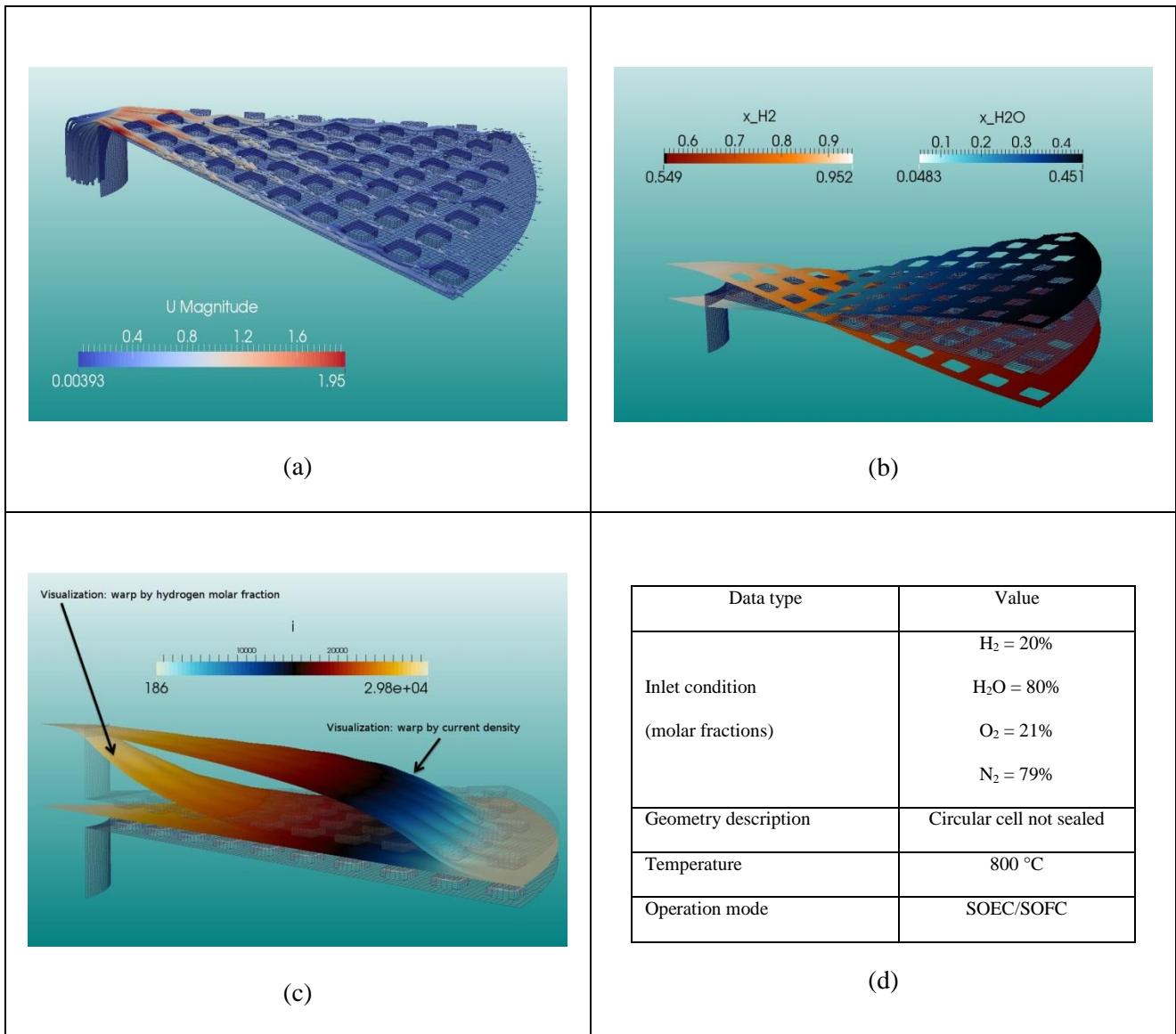

Figure 3: SOC simulation: velocity streamlines (a), species warp (b), current density warp (c) and main operating conditions (d)

Numerical simulations involve many physical parameters that are known with relevant uncertainness. This is due because these parameters are usually measured in ideal conditions far from the real operating conditions. Often in order to tune the models many of these parameters are used as a tuning of "free" parameters to fit the experimental data. This implies that SOC numerical models can usually reproduce very well the existing operating conditions but some difficulties appear when these models are used to design new devices or to predict different operating conditions.

High level models necessarily consider emulated quantities or relations often derived from previous specific simulations in ideal conditions. For this reasons in that kind of numerical simulations need a parametric sensitivity analysis in order to provide the robustness of the results. To obtain results shown in Figure 4 this approach has been used. The used procedure is:

- numerical results are obtained using the parameters set that give the best fit respect to the experimental data;
- then parametric analysis has been performed varying Buttler-Volmer coefficients in using value provided in literature;
- error bars are calculated for voltage and current as the solver can operate both with given total current and with given voltage

As shown in Figure 4 using values provided in literature for Buttler-Volmer equations it is possible fit a wide range of experimental data. This means that this kind of numerical results have poor quality and robustness even if seems adequately match experimental data. This aspect is one of the main lack concerning SOC modeling (10) and are taken into account in the present work. Two prescriptions mays be derived from this:

- numerical results have to be provided with error bars associated to a sensitivity analysis every times they involve emulated parameters/relations;
- in complex SOC models (i.e. a SOC stack model) the added value of the numerical results is to provide a powerful instrument to understand trends and to evaluate difference design and configurations.

Actually the robustness of the numerical results in SOC modeling is too poor in order to obtain significant data from single simulation.
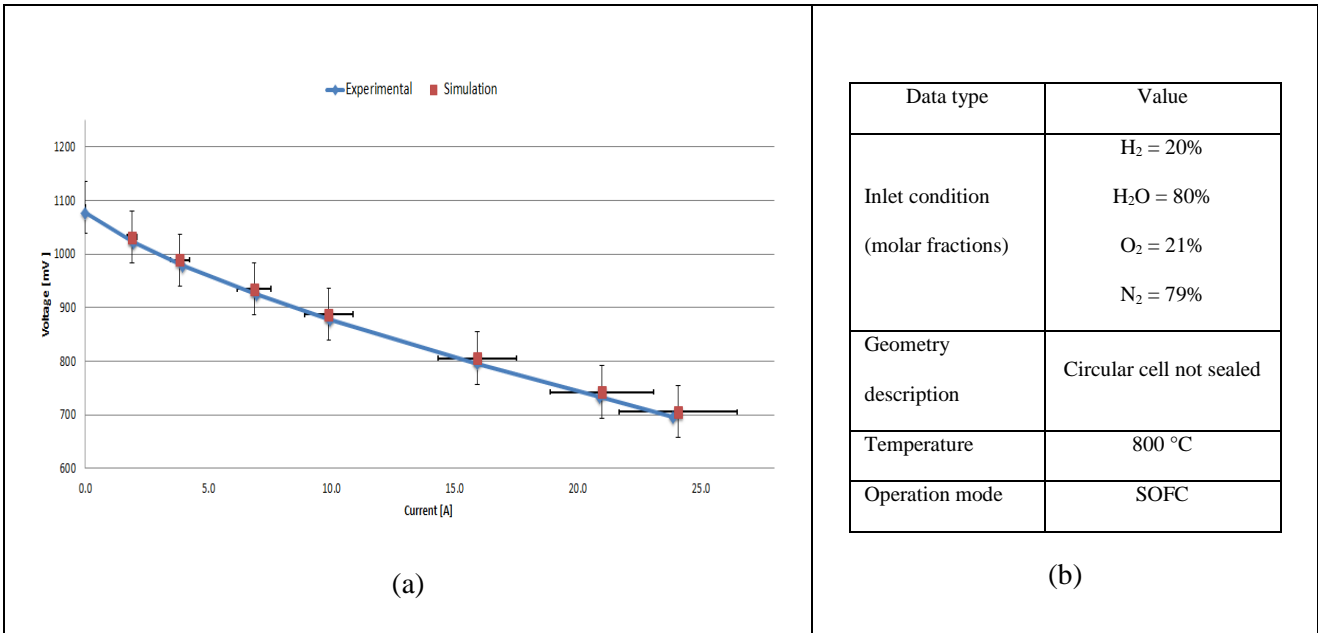
Figure 4: experimental data and numerical results coupled with error bars related to numeric uncertainness (a) and main operating conditions (b)

The new SOC solver developed in the present work can also predict the flow field inside a complete stack. There are no limitations in the model global size (in term of number of elements) as the solver is based on robust open source framework that provide an efficient parallel implementation without any limitations concerning licenses. The simulations done for the present work have been executed using parallelized computation up to 64 processors. In Figure 5 and Figure 6 show vector plot of the velocity field and contour of the temperature field inside a sealed SOC stack. In particular a 10 cell stack operating in fuel cell mode cooled using two heat pipes plates has been simulated in order to test the solver capability concerning thermal sub model and complex thermal boundary conditions handling.
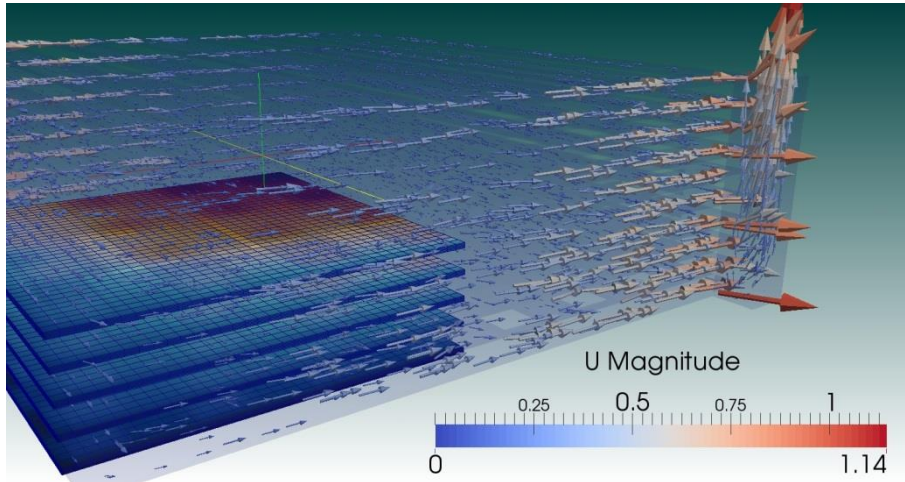
Figure 5: vector plot inside 10 cell stack

The last solver capability that has to be described is the heterogeneous reactions handling. The solver let the user to define both volumetric and surface mass/molar sources. To obtain the sources values the solver uses special sub routine for directly solve the ODE system related to the specified reaction mechanism. For handling more complex mechanism, and in particular heterogeneous mechanisms, it can be coupled with dedicated external tool. Essentially the OpenFOAM solver provides the environment conditions (partial pressures and temperature) to the chemical solver that gives back the calculated mass sources according to the reaction mechanism.
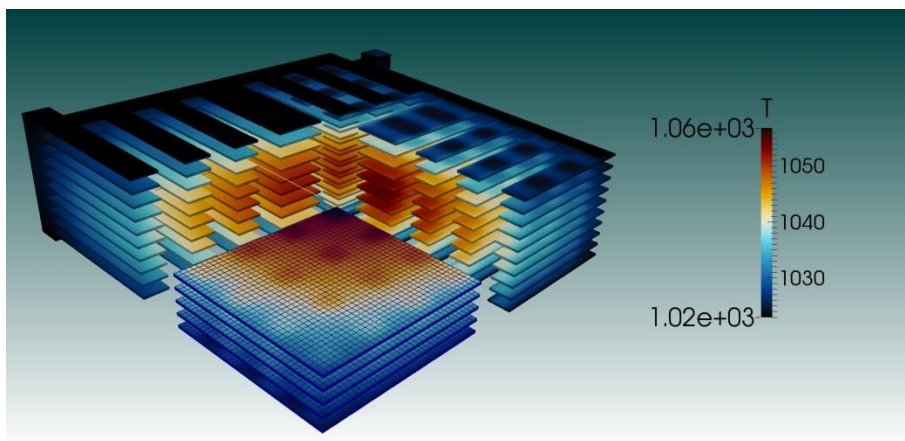
Figure 6: temperature contour inside 10 cell stack

Data type	Value
Inlet condition (molar fractions)	$H_2 = 90\%$ $H_2O = 10\%$ $O_2 = 21\%$ $N_2 = 79\%$
Geometry description	Square cell, 10 cell stack
Temperature	800 °C
Operation mode	SOFC

Table 2: relevant operating conditions referred to case shown in Figure 4 and figure 5

Even if the solver can handle every reaction mechanism particular attention has to be paid concerning the reliability and the robustness of the obtained results. Heterogeneous reactions are phenomena that occur at pore or nano-scales. The two common ways in order to consider these reactions in an high level model is:

(a) model the porous media as a non-continuum differentiating the pore and fluid phases and then applying complex heterogeneous mechanism at the phase interface;

(b) model the porous media as continuum and applying reaction sources as a volume sources, usually considering simplified reactions.

Approach (a) is not practicable in SOC high level models for computational resources issues. Approach (b) is the common used in SOC stack model but in this case the robustness and the accuracy of the results strongly depend by semi-empirical parameters and relations used in the simplified reactions mechanisms.

During the PhD many simulations are set up both using the OpenFOAM standard chemical routines and coupling the new SOC solver with the Cantera tool (11). Unfortunately no appreciable results are been obtained because the tuning of the heterogeneous mechanism used (12) showed a too high sensitivity respect to the active area surface density that cannot be consider a known parameter. For this reason in this works high level SOC models are set up in hydrogen-water configuration only. This limitation is not due to the solver but is related to the SOC modeling in general that need a strong coupling with experimental activity in order to correctly handling the heterogeneous reactions tuning. Figure 7 shows results obtained coupling the

open source in-house developed SOC solver and the Cantera tool. In particular species molar fractions along a SOEC tube are shown. Following SOC modeling prescriptions described before a sensitivity analysis has been done respect to the surface area density that is the main "free" parameter in heterogeneous reaction mechanism. According to the expectations the error bars obtained in this case are extremely relevant so the results cannot be considered reliable.
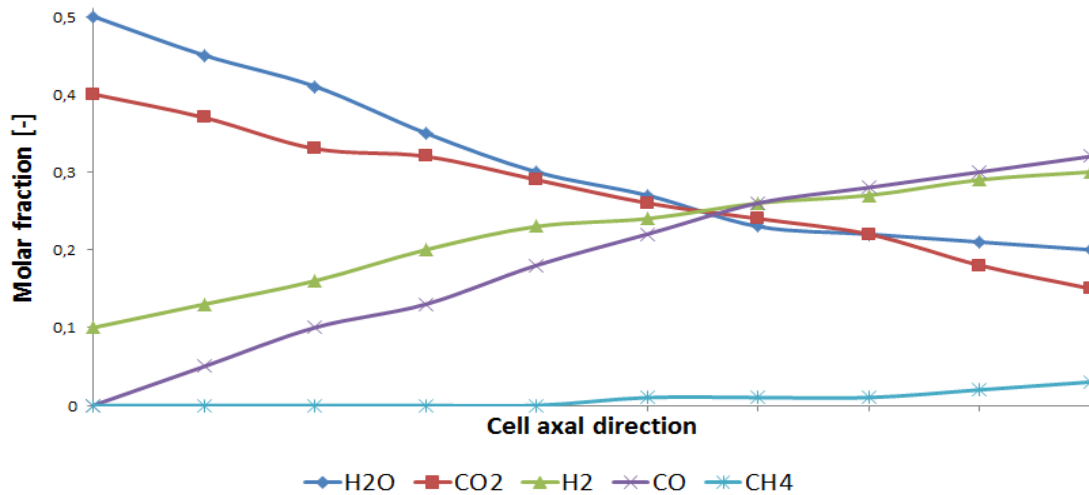

Figure 7: species distribution along inlet-outlet direction inside SOEC device using the best-fit surface area density value

SOC solver: electrochemical impedance modeling

One of the innovative capability of the new SOC solver is that it can compute the electrochemical impedance of a SOC cells and device. The solver can handle in input both a sinusoidal total current or a sinusoidal voltage and perform the simulation over a user defined range of frequencies.

Two main assumptions are considered in the solver:

- hypothesis of non-correlation between high frequency and low frequency processes;

- Nernstian effects are predominant respect to electrochemical ones.

The first hypothesis is the relevant one and justifies the split procedure described later on. In particular, according to this assumption, what happens at high frequency doesn't influence slowest phenomena such as mass transport, temperature transport, etc... This hypothesis has been implemented at numerical level also separating high frequency equations and routines from low frequency ones and the only physical quantity that links low and high frequency phenomena is the local current density. This assumptions is validated

considering that low frequency processes are not affected by the selection of the high frequency models, where current density is calculated, as showed in the rest of the chapter.

The second hypothesis suggests that SOC performances are mainly influenced by the temperature and species distribution along the cell and less influenced by the electrochemical aspects. This assumption is valid in SOC high level model only where kinetic charge transfer and electrochemical phenomena are emulated. This assumption is enhanced by observing the Nernst potential as a function of the fuel utilization, as shown in Figure 8. Comparing the Figure 8 with a typical SOC polarization it is clear that the Nernstian effects represent the leading effects in a solid oxide cell.
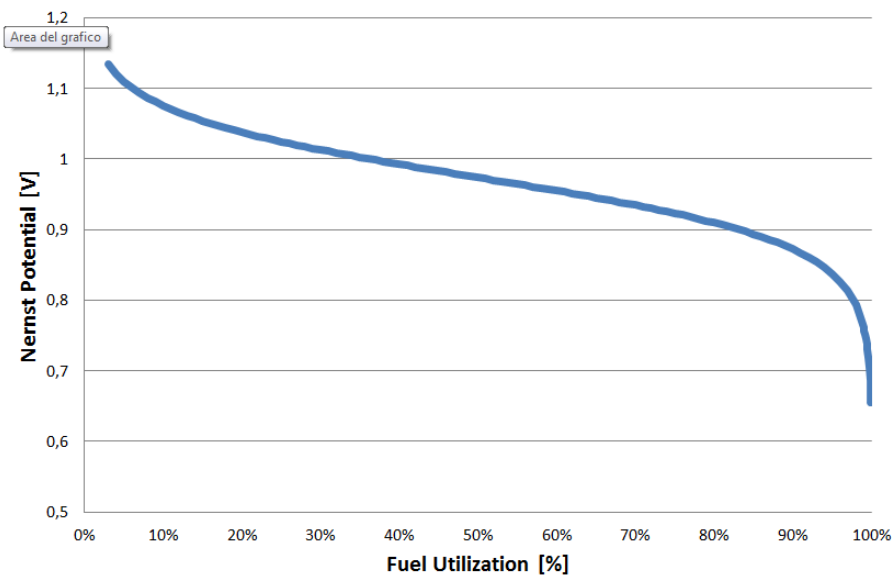
Figure 8: Nernst potential vs. Fuel Utilization (FU)

Nernst equation (3.5) represents how big is the driving force acting on the charge carriers and it is influenced by low frequency processes. On the other hand high frequency phenomena are related to how the driving force influences the system and the charge carriers.

Low frequency processes are the ones characterized by mass transport where the time scales are related to the mass average velocity time scale and to the species gradients time scale. The dynamic response of the low frequency processes is quite complex to be emulated especially when high inhomogeneity occurs. All equations shown in the previous paragraphs are time dependent and they have a different modal response depending on porous media resistance and species concentrations. A typical SOC flow field is characterized by manifolds flow, complex interconnects flow and electrode porous media flow. This implies that 1D

assumptions or quasi-2D assumption (1D trough the electrode thickness and very approximate discretization along the inlet-outlet direction) can't give good quantitative results for low frequency phenomena. This is evident in case of high tridimensional flow (in complex flow distribution or in a complete stack) or in common SOC operation where the inhomogeneity of the species concentrations increase as the reactant utilization increase (13) (14) (15) (16) (17) (18) (19).

High frequency processes are the ones characterized by chemical and electrochemical reactions where the time scales are related to the kinetic of the reactions. As well discussed in (20) and (21), these processes have complex time dependency. The dynamic response of the high frequency processes has been massively investigate especially from an experimental point of view. Many simplified semi-empirical models have been proposed in literature most of them directly defined in the frequency domain. In order to provide a simple model while maintaining an high fidelity reproduction of low frequency processes in the new SOC solver simplified high frequency subroutines are been implemented basing on well-known equivalent circuits used in Electrochemical Impedance Spectroscopy (EIS) (22).

Following the nomenclature defined in previous paragraphs the SOC solver simulates the low frequency processes and emulates the high frequency processes. For predict transport phenomena the solver directly handles the physical partial differential equations while dynamic response of reactions is taken into account using general simplified subroutines defined in frequency domain. Later in in the chapter one of this high frequency subroutine is proposed and detailed description and derivation is provided.

Algorithm description

The computational domain that the solver can handle consists in fully 3D fluid domains representing the inlet and outlet gases manifolds and gas distribution channels both for fuel and air side. Starting from initial conditions, the solver runs until the open circuit voltage (OCV) condition is reached. From this point, transient polarization is performed as described before. Results (temperature fields, species concentrations fields, current density distribution, etc…) are stored for each point of the polarization and an harmonic input (voltage or total current) is provided. The discretization in time is set considering the more stringent condition between $t < \frac{1}{300\,f}$ and $t < t_{CFL}$, where f is the harmonic frequency of the input signal and t_{CFL} is the maximum time step that can guarantee the respect of the numerical Courant-Friedrichs-Lewy (CFL)

condition (23). The time step is variable during the simulation and it is enforced by the CFL condition at low frequencies and by the adequate shape reproduction of the input signal at high frequencies (at least 300 time steps are simulated over an harmonic period).

For each time step all parameters and coefficients are updated and all equations are solved both in all fluid and solid domains in order to provide an updated variables state (temperature and species partial pressures) at the electrolyte interface. Then for each electrolyte computational cell the local Nernst driving force is update. Finally the fields values (temperature, partial pressures, etc…) are provided to the high frequency subroutines that gives in output the local current density and the local species mass/molar consumption/production. For every frequency the simulations have been run for a user defined number of periods of the harmonic input signal. Parametric sensitivity analysis over the number of periods has been done. Numerical results suggest that three periods are enough in order to reach the regime condition. This has been monitored measuring the shift phase between total current and voltage as shown in

Figure 9.
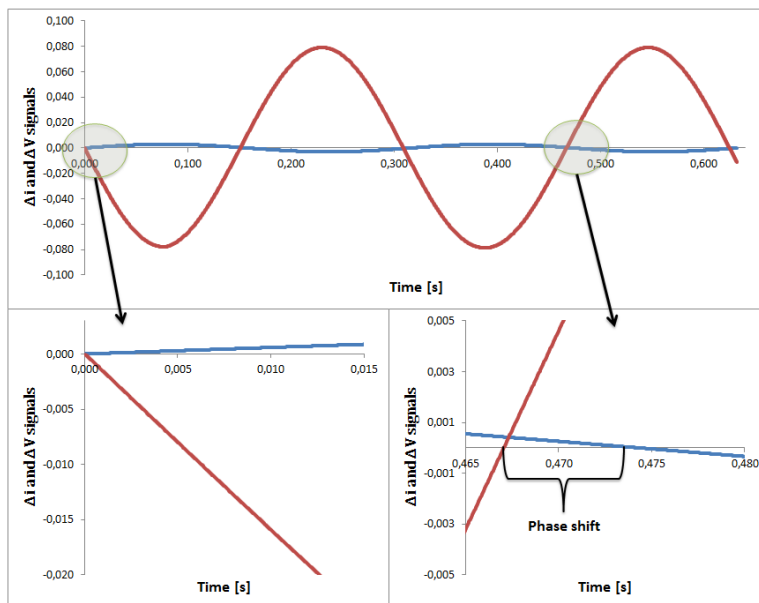
Figure 9: evolution of the phase shift between current and voltage governed by PDEs

Basing on the calculated time shift value and the signals amplitude ration the impedance value is obtained as a complex number. The phase shift due to high frequency processes is obtained at the first time step as it is directly calculated in the frequency domain. The mass transport processes impedance is obtained by the

solver subtracting the impedance value provided by the high frequency subroutines. A schematic representation of the algorithm is reported in Figure 10.
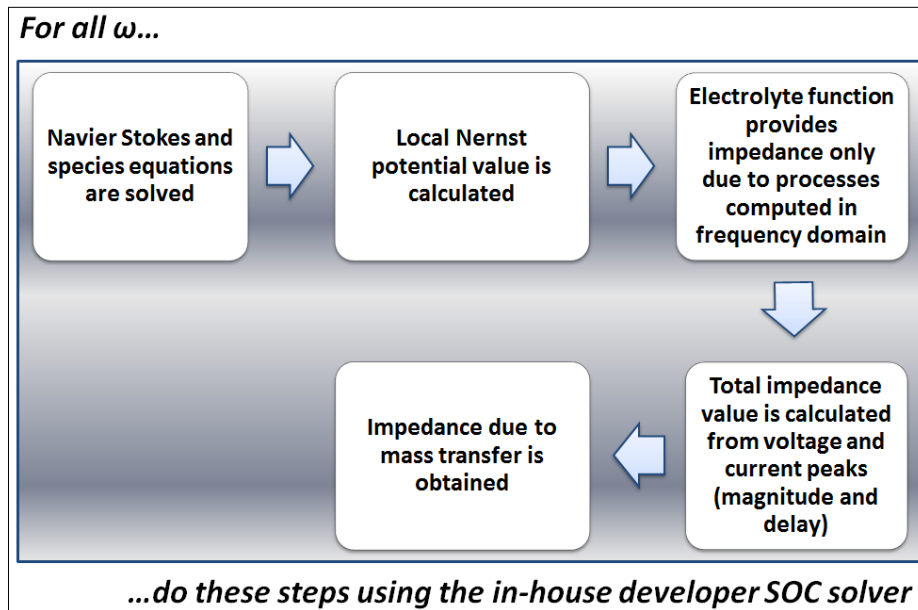

Figure 10: schematic representation of the algorithm for mass transport processes impedance evaluation

The low frequency processes impedances are influenced by geometry of the manifolds and channels by the porous media. In

Figure 11 is shown the physical interface between flow channels ribs and electrode. Regions with poor reactants feed are generated as the porous medium hinders the species diffusion. This "shadow effect" is the main cause of the dynamic behaviour concerning the SOC low frequency processes. The greater is the reactant utilization the greater is the effect related to the species concentration inhomogeneity.
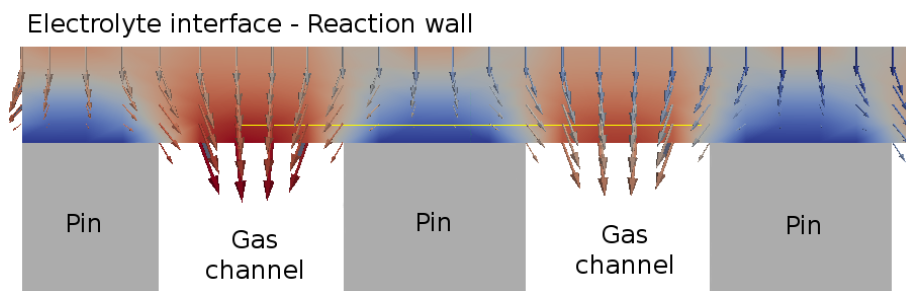

Figure 11: hydrogen concentration is low behind interconnect ribs due to their shadow effect (6)

Impedance spectra calculation

The high frequency phenomena are taken into account by a spatial distributed HF element grid as schematically shown in Figure 12.
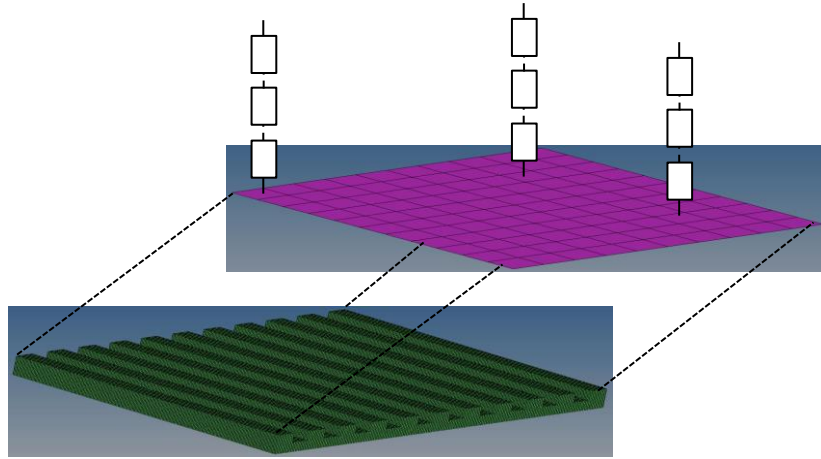

Figure 12: schematic representation of 2D distribution of circuit lines

Solver high frequency performances depend on the choice of the HF equivalent circuit. For the simulations included in the present work a simple equivalent circuit has been used as describer later on. As shown at the end of the chapter even if the HF sub model is very simple the results are quite accurate confirming low frequency processes have a strong impact on SOC devices.

Impedance calculated in SOC is the complex proportionality factor that relates total current and voltage both varying in time. General scheme of the equivalent circuit is represented in Figure 13.
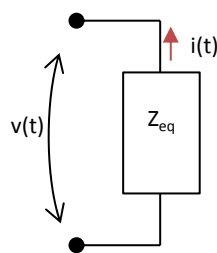

Figure 13: general impedance scheme for SOC

The complete circuit behind the equivalent impedance value Z_{eq} is the one shown in Figure 14. Here impedances Z_{Dan} represent the diffusion related impedances at the air side (dynamic behaviour of fields that

influence Nernst potential at the air side), impedances Z_{Dfn} represent the same quantity at the fuel side and impedances $Z_{En,n}$ represent the n-electrochemical processes that happened in the electrodes and in the electrolyte. In order to simplify the equivalent circuit the links between different circuit lines are supposed to be characterized by infinite resistances. From a physical point of view this implies to neglect the transversal in-plane current density in the electrolyte. In this way each equivalent circuit line is related to a single electrolyte computational cell. This means that for 3D discretization a 2D series of one dimensional line has to be considered as schematically shown in Figure 12.
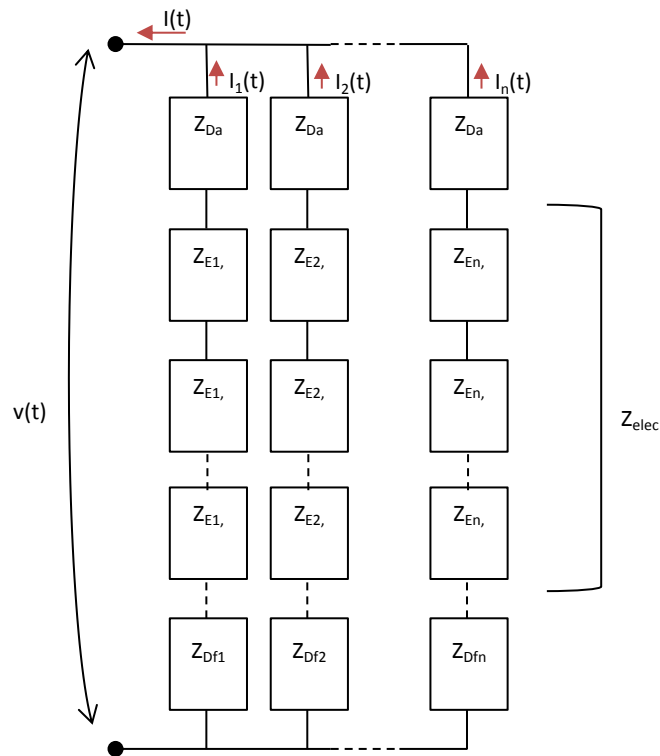

Figure 14: complete SOC equivalent circuit

Introducing the decoupling assumption presented in the previous paragraphs it is possible to derive a simpler equivalent circuit as the one shown Figure 15. At this stage transport equations can be solved independently from the equations implemented in the electrolyte subroutines that can be implemented directly in frequency domain.

At high level the equivalent circuit reduce to the one shown in Figure 16 where Z_{elec} is the parallel of all $Z_{elec,n}$ and Z_{Da} and Z_{Df} are the total impedances related to the air and fuel mass transfer. Concerning the high

frequency processes the developed SOC solver can handle every equivalent circuits that can be rearranged in this form.
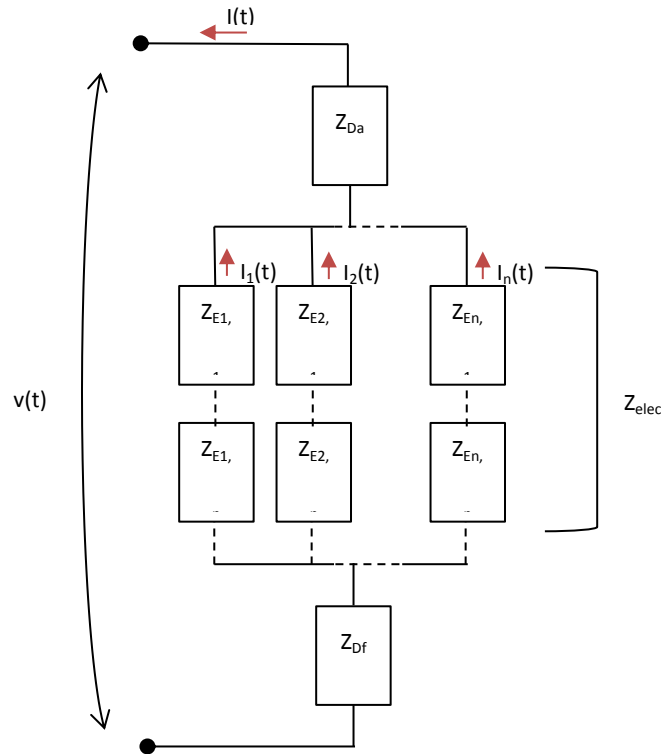

**Figure 15: simplified SOC equivalent circuit**
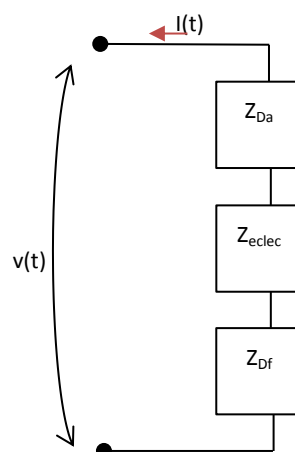
Figure 16: high level simplified SOC equivalent

The reference configuration considered in the solver considers the HF impedance $Z_{elec,n}$ as the series of three pure resistive elements as shown in Figure 17. In particular only the electrolyte resistive contribution and the electrodes nonlinear resistive Buttler-Volmer contributions have been taken into account. This equivalent circuit is implemented in the subroutines used to compute the polarization with constant input signals. Resistances values are function of the local variable distribution and of the operation condition. Resistive contributions are calculated using the follow relations:

$$i = \gamma_f \prod y_j^{\alpha_j} \left[e^{\frac{\vartheta_{f1} \eta_{act,f} F}{RT}} - e^{-\frac{\vartheta_{f2} \eta_{act,f} F}{RT}} \right] \tag{3.6}$$

$$i = \gamma_a \prod y_j^{\alpha_j} \left[e^{\frac{\vartheta_{a1} \eta_{act,a} F}{RT}} - e^{-\frac{\vartheta_{a2} \eta_{act,a} F}{RT}} \right] \tag{3.7}$$

$$\eta_{ohmic} = i R \tag{3.8}$$
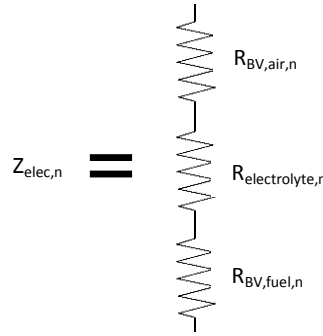
Figure 17: reference configuration equivalent impedance

In the reference configuration the solver can compute impedance related to mass transfer ($Z_{Da} + Z_{Df}$). The solver can compute separately Z_{Da} and Z_{Df} simply by freezing the flow fields respectively in fuel and air side. When the total mass transfer impedance Z_D in known it is possible to combine it with more complex electrodes and electrolyte equivalent circuits taking the advantage to provide them a complete fields distribution along the electrolyte.

In the present works a simple implementation Z_{elec} has been selected as shown Figure 18 where high frequency electrochemical processes are assumed as a combination of non-uniform and non-homogeneous resistive elements and constant capacitive element. The resistive electrode elements are computed with the

non-linear Buttler-Volmer equation while the resistance related to the electrolyte is a function of the temperature only.
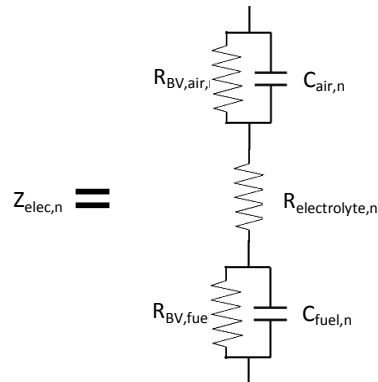

Figure 18: simple configuration of high frequency processes

Numerical setup

In order to validate this solver capability a real experimental setup has been reproduced (24). The setup consists in a sealed ceramic housing (Figure 19 and Figure 21) with channel-rib flow field distribution. Fuel enters from three holes placed on the left side and exits from same number of holes placed on the other side. The cell (Figure 20) divides the fuel and air domains and a glass sealing has been used in order to prevent gas leakages.

Figure 19: fuel housing with flow field distribution
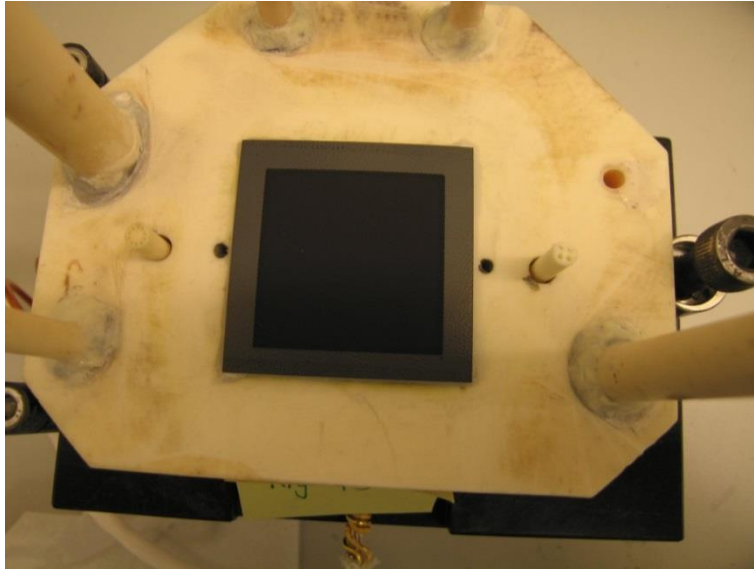
Figure 20: the SOC cell considered in the simulations
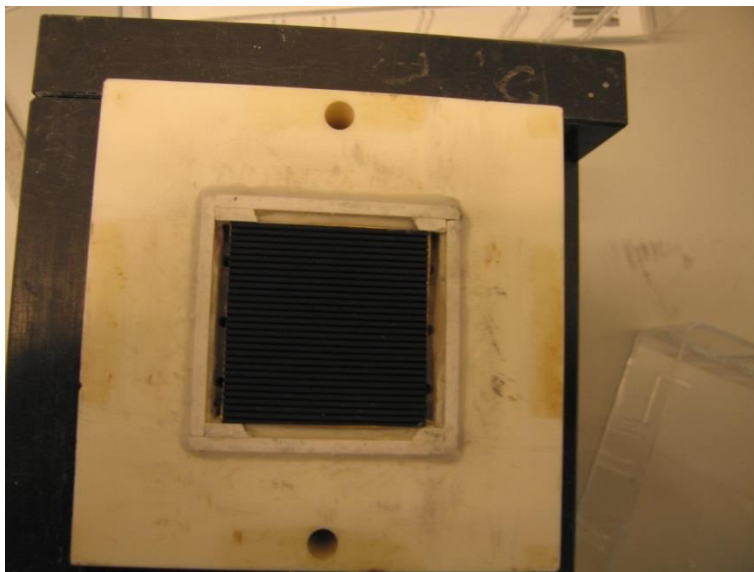
Figure 21: oxidant housing with flow field distribution

The dimensions of the flow channels and interconnect ribs are different between the two sides and a detailed view is shown in Figure 22.
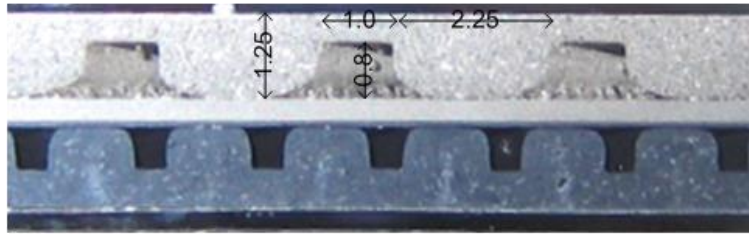
Figure 22: gas channels geometry details

The experimental setup[1] has been reproduced using SolidWorks® tool (25) and the geometry de-featuring has been performed in order to obtain the fluid volume as shown in Figure 23. The electrolyte is reproduced as a thin interface where electrochemical processes take place.
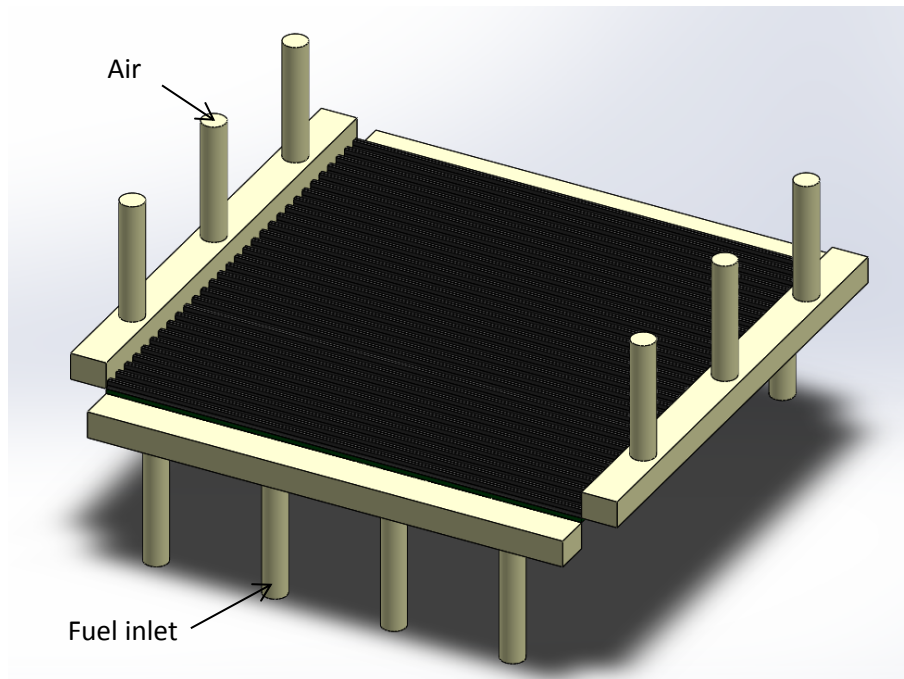

Figure 23: 3D solid model of fluid domains

---

[1] All information concerning experimental data (experimental setup, measurements, data, etc…) come from the period that author has spent in Risø National Laboratory, Roskilde, Denmark. Raw data are provided by professor Henrik Lund Frandsen and professor Christopher Graves and all credits have to be acknowledged to them.
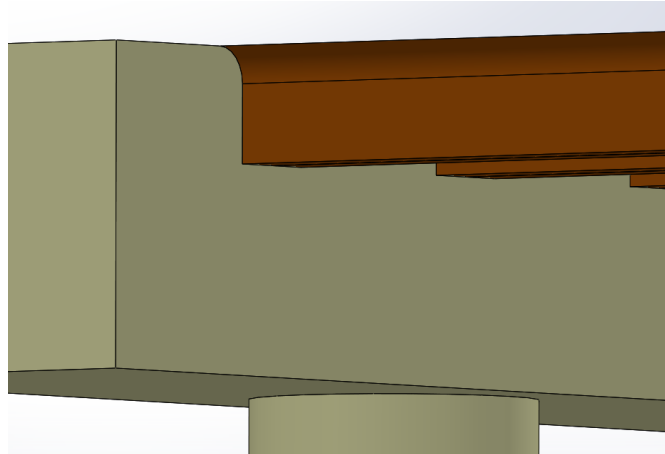
Details concerning boundary conditions are reported inTable 3 and the summary of the relevant operating conditions is shown in Table 4. Cables losses are supposed to be negligible according with the experimental data that come filtered this contribution.

	Inlets	Outlets	Electrolyte interface	Other boundaries
Species mass fractions	Fixed fluxes (Fixed value)	Zero diffusive flux (Zero gradient)	Fixed flux (Faraday equation)	Zero flux
Mass average velocity	Fixed value (Fixed flux)	Zero gradient	Non sip condition	Non sip condition
Pressure	Zero gradient	Fixed Value	Zero gradient	Zero gradient
Temperature	Fixed value	Zero diffusive flux (Zero gradient)	Fixed flux	Adiabatic or external heat exchange

Table 3: boundary conditions

Second order divergence schemes has been used and numerical limiter have been adopted for enthalpy, velocity and species mass fraction convective terms. Second order conservative discretization has been used for diffusive terms as well. Concerning time scheme first order bounded implicit scheme has been used. Preconditioned conjugated gradient linear solver has been used for all sparse matrices except for the pressure equation (Poisson equation) that has been solved using a geometric-algebraic multi-grid (GAMG) approach.

Details of the implementation of these algorithms can be found in (26). Common relaxation factors for velocity, pressure and other variables have been chosen (27) (5).

Data type	Value
Inlet condition (molar fractions)	H_2 = 97% H_2O = 3% O_2 = 21% N_2 = 79%
Geometry description	Square cell, 16 cm^2
Temperature	800 °C
Operation mode	SOFC

Table 4: relevant operating conditions referred to the validation case of the impedance calculation capability

Figure 25 shows experimental data and numerical data related to the low frequency process only. The shapes of the spectra are quite similar and appreciable results are obtained far from OCV also.

For a quantitative solver validation a comparison with experimental data has been done. In Figure 26 results at low fuel utilization are shown. The low frequency arc of the spectrum perfectly fits the experimental data. Also the high frequency part fits quite well the experimental values confirming that in this conditions also a very simple high frequency model could be used.
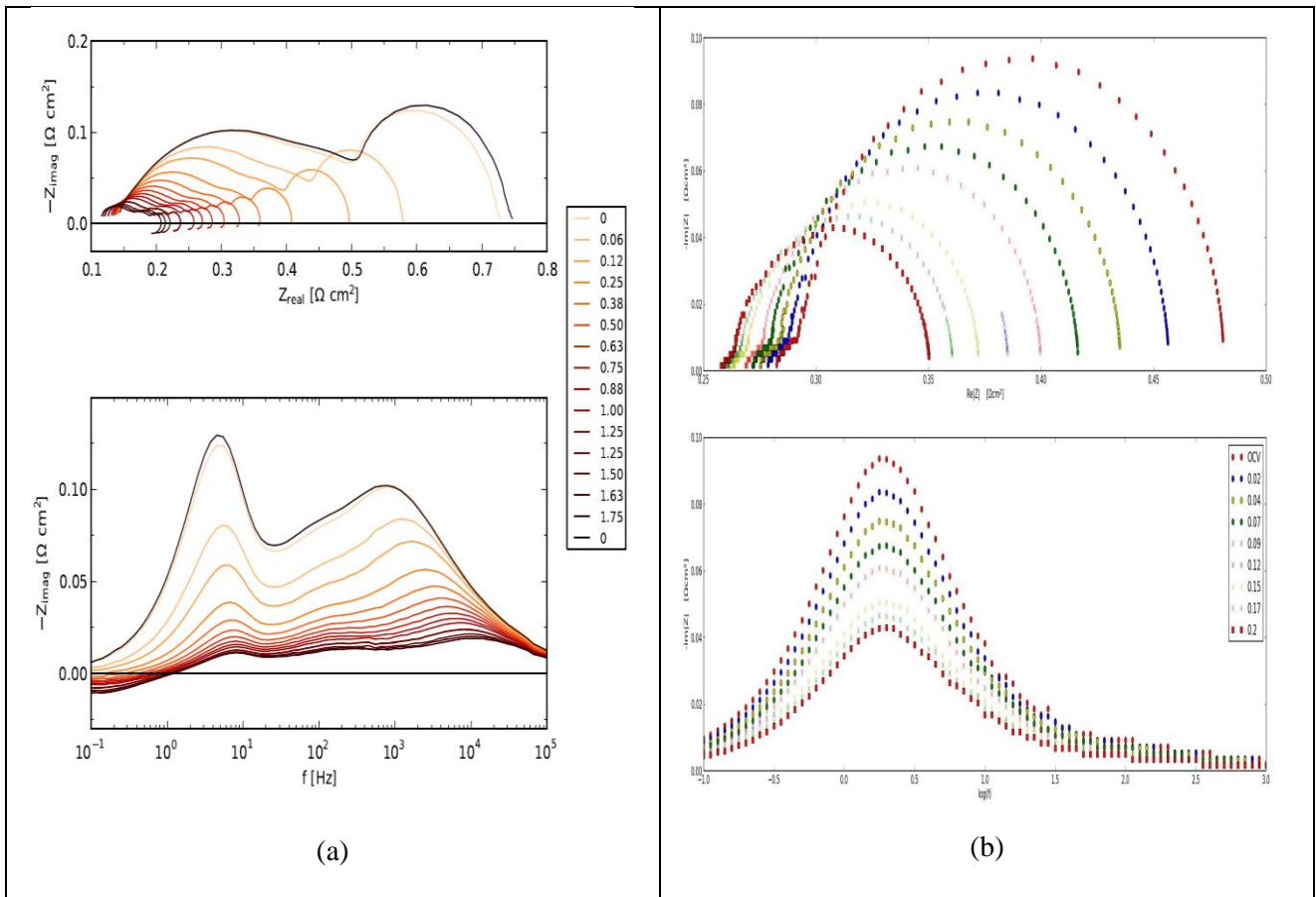
Figure 25: experimental data (a) and numerical results (b) qualitative validation

As shown in Figure 27 the same simulation has been performed only activating low frequency processes. Here the numerical data overlap very well the experimental data and this is due only because the right 3D geometry domains are considered. Switching off the high frequency routines it is possible to emphasise the impedance related to the manifolds represented by a small arc at medium frequency.

At high fuel utilization the low frequency processes still fit well the experimental data while some differences in the high frequency arcs are present as shown in Figure 28. This is due to the choice of a simple HF submodel and results can be improved using more detailed HF routines.

Low FU
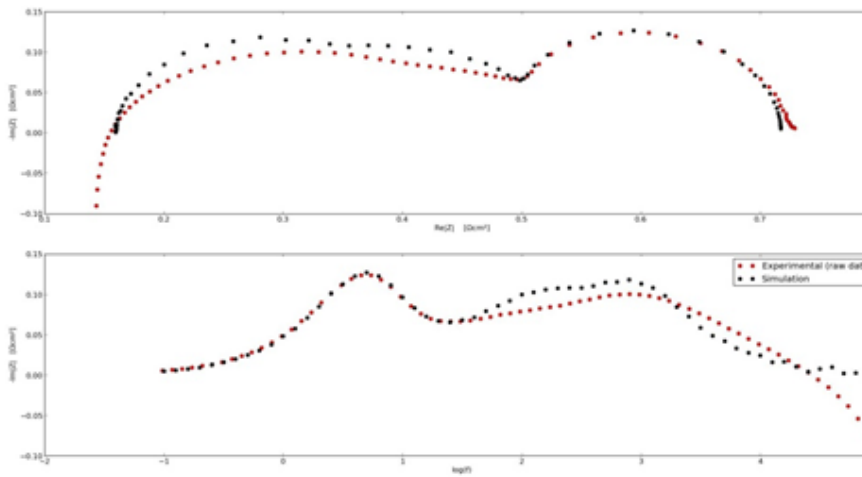
Figure 26: solver quantitative validation

Low FU – LF only
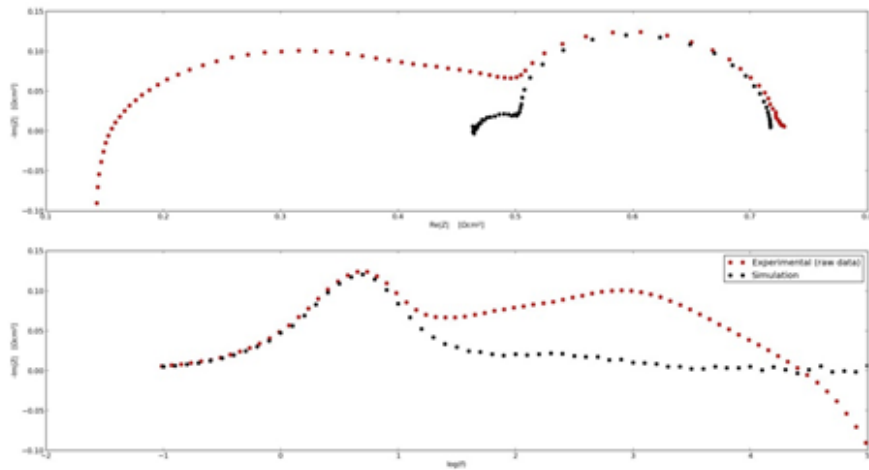
Figure 27: solver quantitative validation – low frequency arc
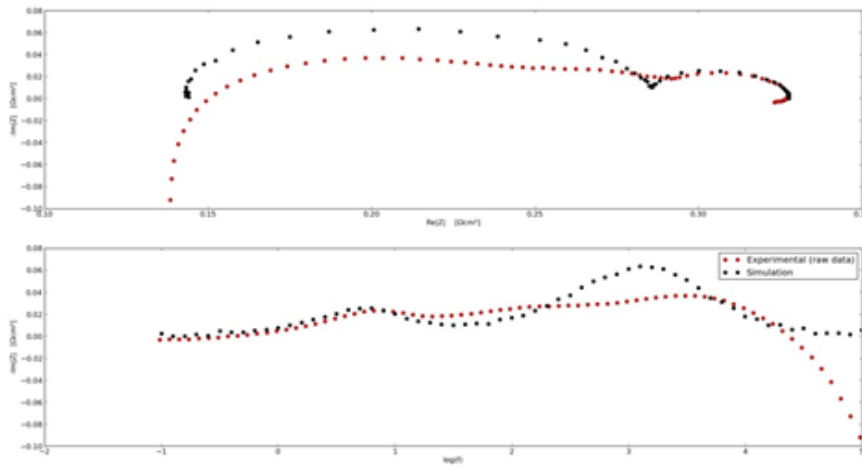
Figure 28: EIS hybrid model at high fuel utilization

Once the solver has been validated some numerical analysis have been performed in order to derive some design prescriptions or in order to investigate certain SOC phenomena. Simulations have been also performed considering geometry with and without solid ribs as shown in Figure 29.
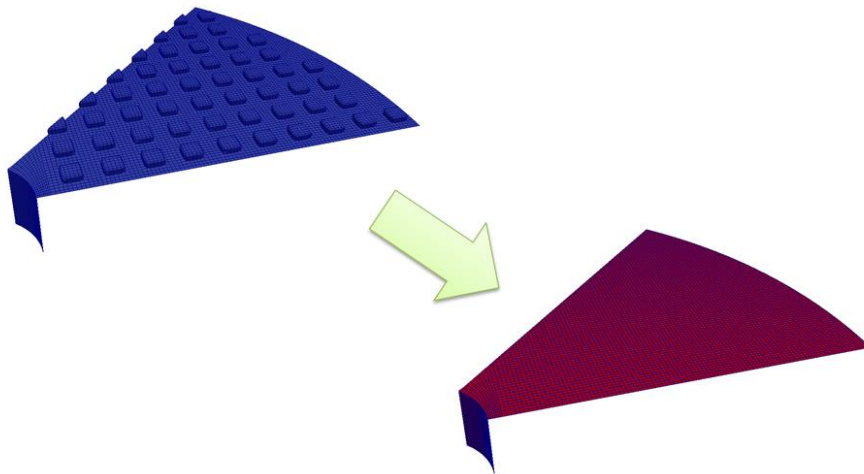
Figure 29: Geometry considered for sensitivity analysis respect to solid pins/ribs

At low fuel utilization there are no appreciable differences in the low frequency part of the spectrum as shown in Figure 30. When the fuel utilization increases some differences appears as shown in Figure 31 and

Figure 32. In particular in presence of solid pins there is a small shift toward the high frequency. This is due to the speedup of the species diffusion processes related to the species gradients that are greater in the geometry with pins ("shadow effect").
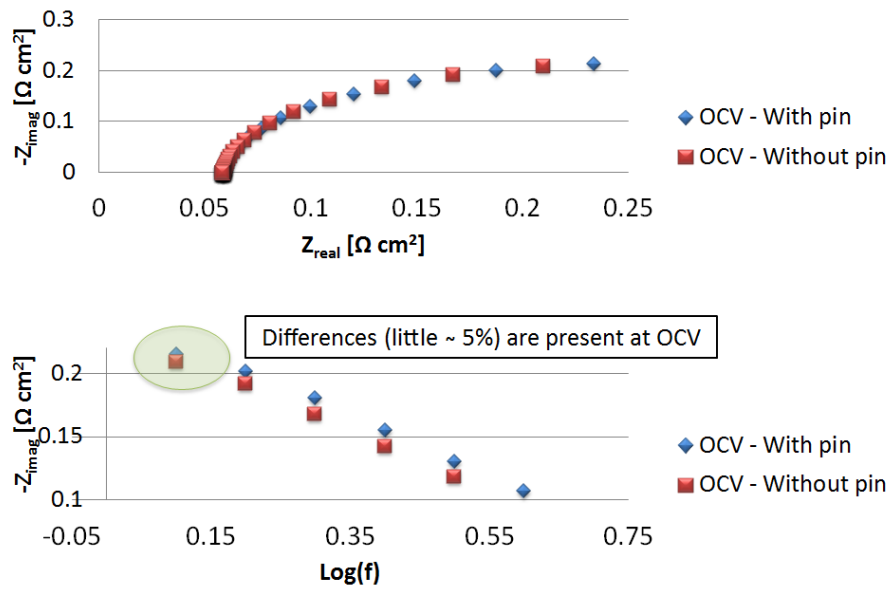
Figure 30: Low frequency process with different geometry (OCV)
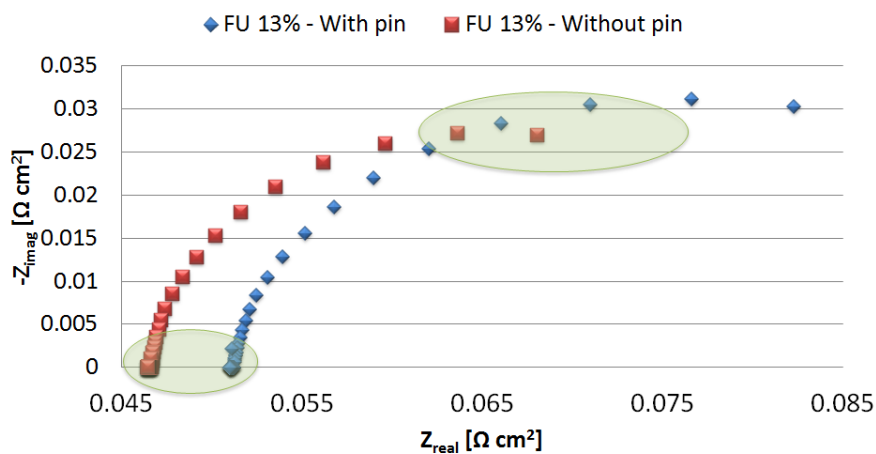
Figure 31: Low frequency process with different geometry (FU = 13%) – Complex plane
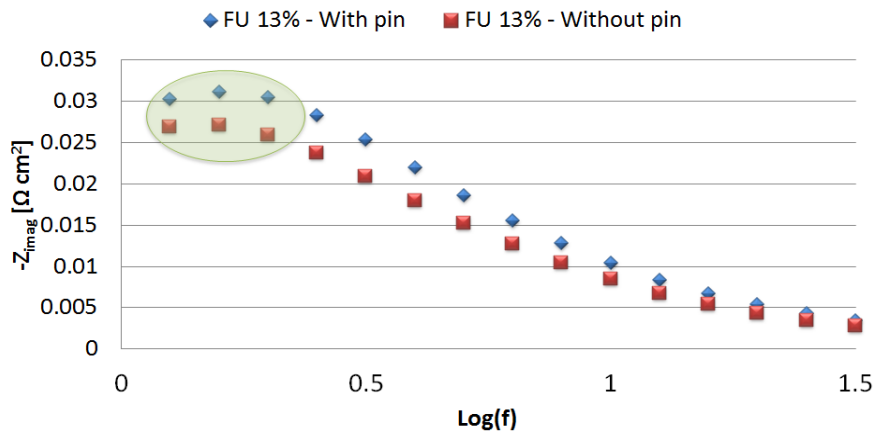
Figure 32: Low frequency process with different geometry (FU = 13%) – Bode phase diagram

Additional simulations have been performed varying the gas channel widths as shown in Figure 33. According to what expected the impedance obtained without any geometrical obstacles in the gas domains is the lowest and 2D models are equivalent in term of accuracy. The impedance varies when geometrical obstacles (ribs) are introduced and increase as the ribs width increases (the gas channels width decreases). In this conditions approximate models or 2D models that don't take into account the exact fluid domains can't provide accurate results and the impedance related to the mass transfer processes is under estimated.
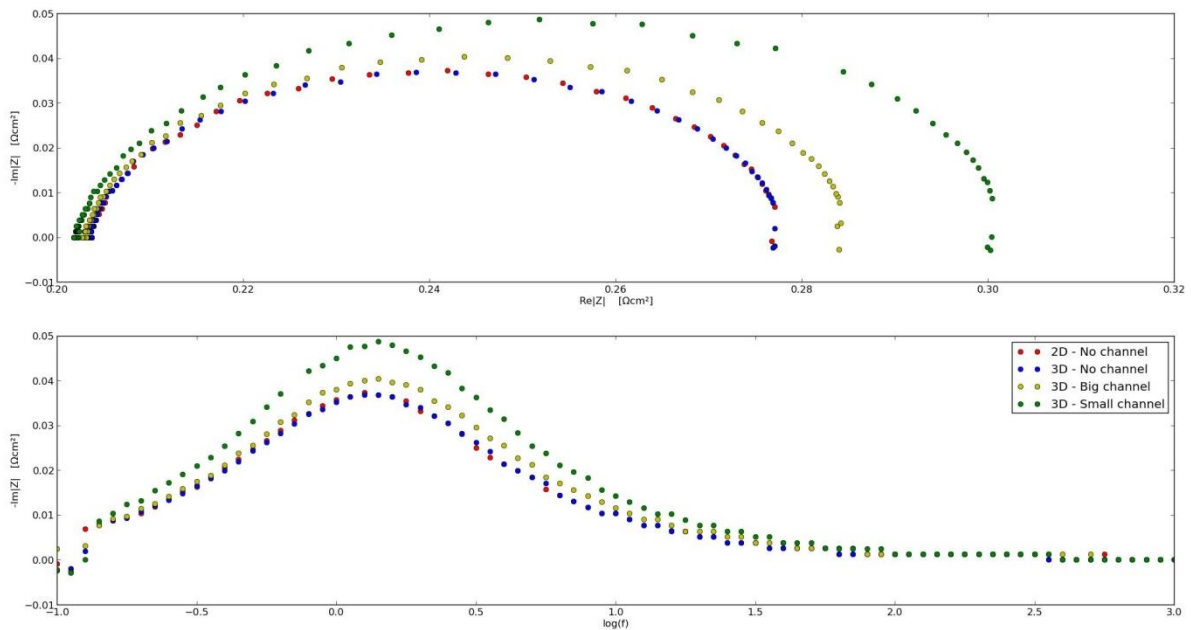
Figure 33: Low frequency spectrum for different gas channels (FU = 75%)

Another important results obtained with this model and this solver concerns the very high frequency part of the spectrum. Usually in literature the intersection between the impedance arc and real axis is consider an estimation of the ohmic resistance of the cell mainly due to the electrolyte resistivity. Numerical results obtained with the new SOC solver show that this resistance is not only due to homic effects (Figure 34). In fact an isothermal simulation has been set up in order to keep constant the ohmic resistance. Contrary to the expectations in some operating conditions when the fuel utilization increases the intersection between the impedance spectrum and the real axis moves toward left producing a sort of fictitious resistance reduction. Hence the simulations suggest that this effect is not only caused by the electrolyte heating but is also due to the resistance caused by diffusion losses.
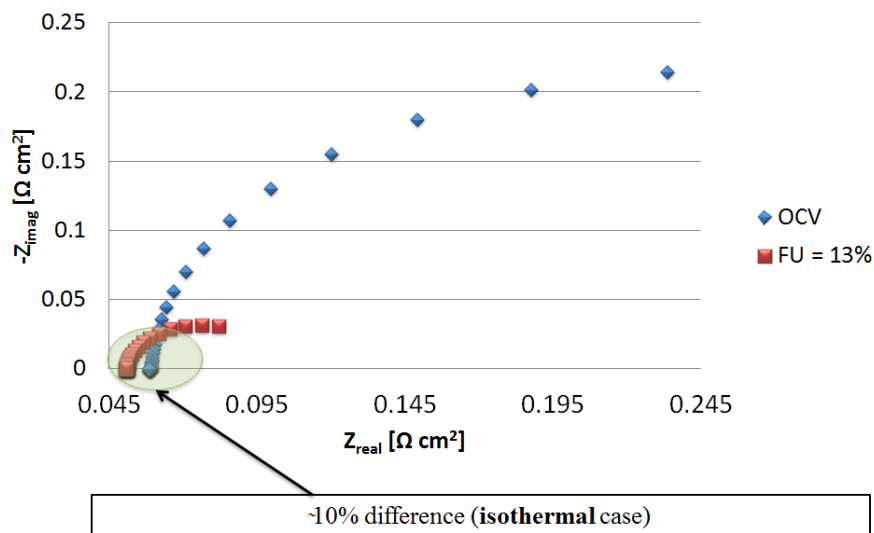
Figure 34: High frequency behavior of the physical simulated arc

This phenomenon was experimentally verified when oxygen utilization is relevant in sealed devices as shown in Figure 25. From an analytical point of view the non-linearity of the Nernst equation produces a non-trivial current density distribution that influences the resistance of the device defined as the ratio between voltage and total current. Figure 35 shows the main data of a 1D calculus in a simple domain divided in three computational cells only where this phenomenon can be reproduced.

$$x_{O2} = 21.00\ \% \qquad x_{O2} = 21.00\ \% \qquad x_{O2} = 21.00\ \%$$

$$V_{OCV}$$

$i_1 \qquad i_2 \qquad i_3$

$\eta_1 \qquad \eta_2 \qquad \eta_3$

$$R^{OCV}_{\ g} = \frac{\Delta V}{\Delta \sum_k i_k}$$

$x_{H2} = 90.00\ \% \qquad x_{H2} = 89.99\ \% \qquad x_{H2} = 89.98\ \%$

$x_{H2O} = 10.00\ \% \qquad x_{H2O} = 10.01\ \% \qquad x_{H2O} = 10.02\ \%$

$\eta_1 = 0.51$ mV $\qquad \eta_2 = 0{,}45$ mV $\qquad \eta_3 = 0.40$ mV

$$R^2_{\ \Omega} < R^1_{\ \Omega}$$

$x_{O2} = 21.00\ \% \qquad x_{O2} = 20.95\ \% \qquad x_{O2} = 21.90\ \%$

$$V_{0.9}$$

$i_1 \qquad i_2 \qquad i_3$

$\eta_1 \qquad \eta_2 \qquad \eta_3$

$$R^{0,9}_{\ g} = \frac{\Delta V}{\Delta \sum_k i_k}$$

$x_{H2} = 90.00\ \% \qquad x_{H2} = 84.30\ \% \qquad x_{H2} = 79.15\ \%$

$x_{H2O} = 10.00\ \% \qquad x_{H2O} = 15.70\ \% \qquad x_{H2O} = 20.85\ \%$

$\eta_1 = 245.51$ mV $\qquad \eta_2 = 221{,}56$ mV $\qquad \eta_3 = 205.49$ mV
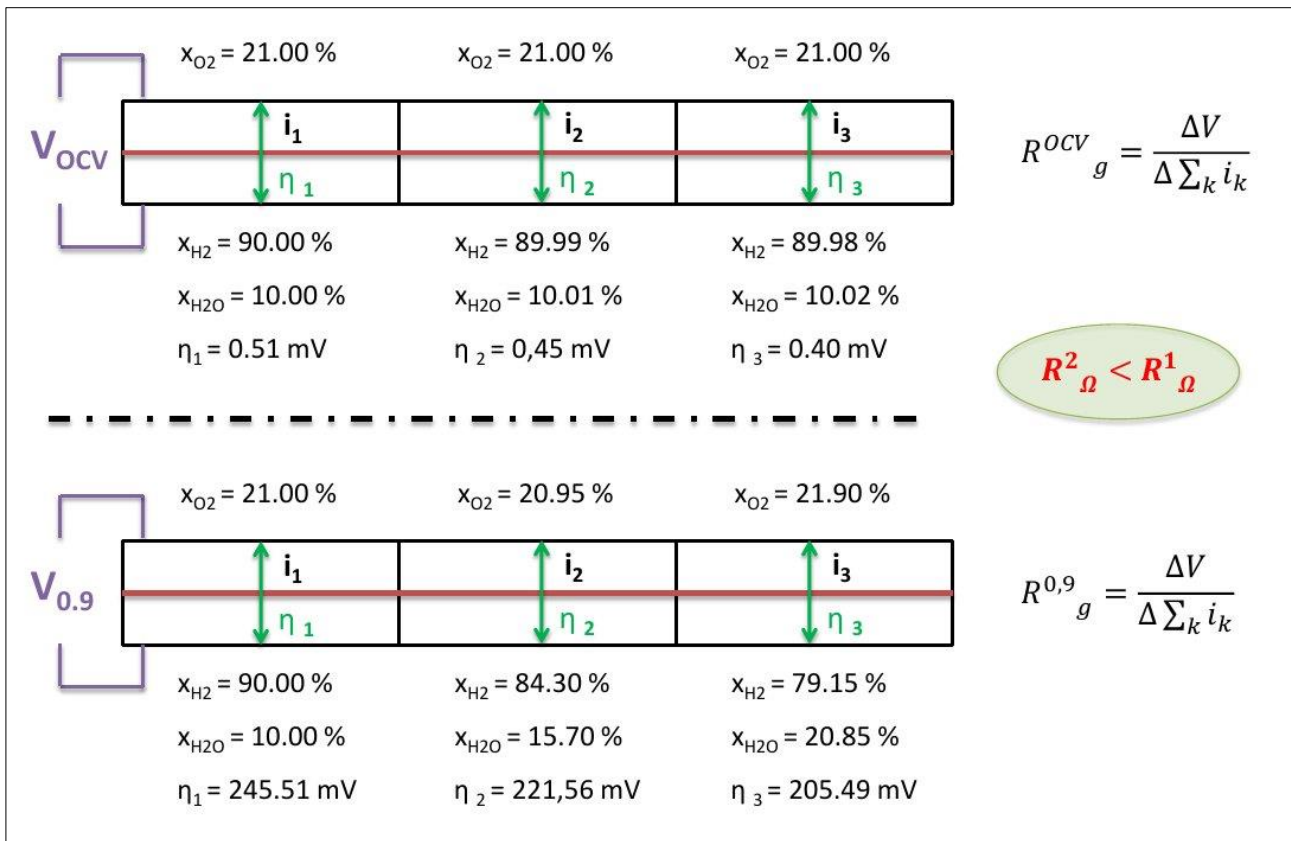
Figure 35: Schematic representation of the fictitious ohmic resistance reduction

This effect can be quite important because usually the shift of the spectrum measured increasing the fuel utilization (increasing the total current) is interpreted only as a reduction of the electrolyte resistivity caused by heating and the these data are often used to compute the dependence respect to the temperature of the electrolyte resistivity.

Conclusions

In this chapter numerical modeling approach concerning the solid oxide cell was presented. At the beginning some concepts have been in order to underline the main issues and the main limitations in SOC modeling. Then the mathematical model was defined detailing equations and relations that govern the different physical processes. It has been emphasized that high level models for SOFC and models for SOEC only differ in the implemented heterogeneous mechanisms because the aspects that have to be handled are identical.

The chapter continues with the description of the in-house developed SOC open source solver based on OpenFOAM®. First the solver capability to predict the polarization curve both for SOFC and SOEC has been shown. Then the innovative solver capability to directly simulate the low frequency SOC impedance spectra has been described. In order to demonstrate the improvements related to the fully 3D geometry handling a quantitative validation of the solver has been performed with experimental data. At the end the solver has been used to show the influences of the physical obstacles or occlusions inside the fluid domains. Furthermore some simulations in isothermal condition have been performed in order to emphasize an explanation of a physical behavior commonly attributed to other causes.

1. **Asinari, P. e Chiavazzo, E.** *An Introduction to Multiscale Modeling with Applications.* 2013. p. 99-115. Vol. 47, Asia-Pacific Forum on Renewable Energy 2011 . ISSN: 0360-5442 DOI: http://dx.doi.org/10.1016/j.energy.2012.08.047.

2. *SOFC mathematic model for systems simulations - Part one: from a micro-detailed to macro-black-box model.* **Bove, Roberto, Lunghi, Piero e Sammes, Nigel M.** 2, 2005, International Journal of Hydrogen Energy, Vol. 30, p. 181-187. Fuel Cells . ISSN: 0360-3199 DOI: http://dx.doi.org/10.1016/j.ijhydene.2004.04.008.

3. *SOFC mathematic model for systems simulations - Part 2: definition of an analytical model.* **Bove, Roberto, Lunghi, Piero e Sammes, Nigel M.** 2, 2005, International Journal of Hydrogen Energy, Vol. 30, p. 189-200. Fuel Cells . ISSN: 0360-3199 DOI: http://dx.doi.org/10.1016/j.ijhydene.2004.04.018.

4. **Singhal, S., Kendal, K.** *Solid Oxide Fuel Cells.* s.l. : Elsevier.

5. **Versteeg H.K., Malalasekera W.** *An introduction to Computational Fluid Dynamics: The Finite Volume Method.* s.l. : Pearson Education Limited, 2007.

6. *An open-source library for the numerical modeling of mass-transfer in solid oxide fuel cells.* **Novaresio, Valerio, et al., et al.** 1, 2012, Computer Physics Communications, Vol. 183, p. 125-146. ISSN: 0010-4655 DOI: http://dx.doi.org/10.1016/j.cpc.2011.08.003.

7. *Gas Transport in Porous Media: The Dusty-Gas Model.* **Mason, E. e Malinauskas, A.** New York : Elsevier, 1983.

8. OpenFOAM. [Online] http://www.openfoam.org.

9. Foam-extend. [Online] http://www.extend-project.de/.

10. **Enea.** Workshop "Integrating numerical and experimental approaches for the design of next generation fuel cells". Rome : s.n., 10 December 2013.

11. **Cantera.** [Online] http://cantera.github.io/docs/sphinx/html/index.html.

12. **Deutschmann, O.** Detchem. [Online] http://www.detchem.com/.

13. *Direct two-dimensional electrochemical impedance spectra simulation for solid oxide fuel cell* . **Shi, Yixiang, Wang, Hongjian e Cai, Ningsheng.** 0, 2012, Journal of Power Sources , Vol. 208, p. 24-34. ISSN: 0378-7753 DOI: http://dx.doi.org/10.1016/j.jpowsour.2012.02.012.

14. *Simulation of EIS spectra and polarization curves based on Ni/YSZ patterned anode elementary reaction models.* **Shi, Yixiang, Cai, Ningsheng e Mao, Zongqiang.** 1, 2012, International Journal of Hydrogen Energy , Vol. 37, p. 1037-1043. 11th China Hydrogen Energy Conference . ISSN: 0360-3199 DOI: http://dx.doi.org/10.1016/j.ijhydene.2011.03.019.

15. *Mechanistic model based multi-impedance curve-fitting approach for solid oxide fuel cells* . **Shi, Junxiang e Xue, Xingjian.** 1, 2011, Journal of Electroanalytical Chemistry , Vol. 661, p. 150-156. ISSN: 1572-6657 DOI: http://dx.doi.org/10.1016/j.jelechem.2011.07.034.

16. *Impedance of SOFC electrodes: A review and a comprehensive case study on the impedance of LSM:YSZ cathodes.* **Nielsen, Jimmi e Hjelm, Johan.** 0, 2014, Electrochimica Acta, Vol. 115, p. 31-45. ISSN: 0013-4686 DOI: http://dx.doi.org/10.1016/j.electacta.2013.10.053.

17. *Detailed dynamic Solid Oxide Fuel Cell modeling for electrochemical impedance spectra simulation* . **Hofmann, Ph. e Panopoulos, K.D.** 16, 2010, Journal of Power Sources , Vol. 195, p. 5320-5339. ISSN: 0378-7753 DOI: http://dx.doi.org/10.1016/j.jpowsour.2010.02.046.

18. *A review of AC impedance modeling and validation in SOFC diagnosis.* **Huang, Qiu-An, et al., et al.** 28, 2007, Electrochimica Acta , Vol. 52, p. 8144-8164. ISSN: 0013-4686 DOI: http://dx.doi.org/10.1016/j.electacta.2007.05.071.

19. *Solid oxide electrolysis cell analysis by means of electrochemical impedance spectroscopy: A review.* **Nechache, A., Cassir, M. e Ringued, A.** 0, 2014, Journal of Power Sources , Vol. 258, p. 164-181. ISSN: 0378-7753 DOI: http://dx.doi.org/10.1016/j.jpowsour.2014.01.110.

20. *A new computational approach for SOFC impedance from detailed electrochemical reaction diffusion models.* **Bessler, Wolfgang G.** 11â€"12, 2005, Solid State Ionics, Vol. 176, p. 997-1011. ISSN: 0167-2738 DOI: http://dx.doi.org/10.1016/j.ssi.2005.01.002.

21. *Performance simulation of current/voltage-characteristics for SOFC single cell by means of detailed impedance analysis.* **Leonide, A., et al., et al.** 17, 2011, Journal of Power Sources , Vol. 196, p. 7343-7346. Proceedings of 2010 European Solid Oxide Fuel Cell Forum . ISSN: 0378-7753 DOI: http://dx.doi.org/10.1016/j.jpowsour.2010.10.052.

22. **Orazem, M. E. and Tribollet, B.** *Electrochemical Impedance Spectroscopy.* Hoboken : John Wiley & Sons, 2008.

23. *On the Partial Difference Equations of Mathematical Physics.* **Courant, R., Friedrichs, K. and Lewy, H.** 2, March 1967, IBM Journal of Research and Development, Vol. 11, pp. 215,235.

24. **Jensen, Søren Højgaard.** Solid Oxide Electrolyser Cell. *Risø-PhD-29.* Risø National Laboratory, Roskilde : s.n., December 2006.

25. SolidWorks®. [Online] http://www.solidworks.it.

26. OpenFOAM® User Guide - Numerical schemes. [Online] http://www.openfoam.org/docs/user/fvSchemes.php#x20-1070004.4.

27. OpenFOAM® User Guide - Solution and Algorithm Control. [Online] http://www.openfoam.org/docs/user/fvSolution.php.

Chapter 4
Innovative SOEC stack design

Outline

In this chapter the new SOEC stack design developed during the PhD activity is presented. First an overview of the state of the art concerning the designs is reported in order to show the potentialities and the limitations of the present technologies. The two typical stack configurations (tubular and planar) are described focusing on their advantages and disadvantages. In particular a critical analysis of the different priorities between SOFC and SOEC was performed. A Further discussion on techno-economic aspects concerning the SOC stacks is then reported.

Basing on the criticalities recognition a new SOEC stack design has been proposed. First detailed explanation of the designing process involving interaction between SOC needs and industrial needs is presented. At the end definitive technical drawings of each component is provided with some descriptions concerning materials and machinability.

In order to show the improvements of the new stack design some simulations have been done using the in-house developed solver presented in Chapter 3. In particular the high reactants utilization achievable, the current density distribution improvement and the better thermo-mechanical behavior are shown.

Stack specifications

Solid oxide cells have been studied from many decades (1). One of the most attractive characteristic of these electrochemical devices consists in their high operating temperature. This temperature lets to avoid expensive catalytic materials and promotes the hydrocarbon cracking and recombination. Furthermore high enthalpy exhausts can be obtained and the SOC devices can be coupled with other devices in order to recover the wasted head produced by other processes for reactants pre heating. Unfortunately high temperature has

deleterious impact on materials stability and devices handling. In order to obtain stable SOFC rigs in the last years a compromise has been adopted and the typical stack operating temperature has been reduced up to 600 °C (2). Research concerning cells materials has given a relevant contribution in order to reach these results. Now day many companies and research centers provide quite stable SOFC devices with good performances and acceptable life time. In SOFC operating mode the improvements in cells materials compensate the efficiency reduction due to the temperature decreasing and medium-low temperature SOC devices represent the right compromise. Unfortunately in SOEC operating mode this solution is not acceptable because even if improvements in cells materials take place, the efficiency is dominated by the amount of electric energy that has to be provided to reactants. As shown in chapter 2 this energy demand decreases as the temperature increases. In SOFC the decreasing of the temperatures has the advantage to bypass some technological problems related to the stack assembly. Contrary in SOEC the stack design has to be simplified as much as possible in order to minimize the technological issues due to the high temperatures.

As described in Chapter 2 the capital costs of SOC devices has to be dramatically reduced in order to reach real opportunities on the world market. Now day the capital cost of common SOC stack prototypes is mainly composed in equal parts by cells cost, auxiliaries cost and other materials and processes not elsewhere included (3). Cells costs are related to manufacturing technical aspects and production volumes and the stack design doesn't have big influences upon this. The only prescription that has to be taken into account is the cells shape which the stack is designed for. Circular cells have to be avoided in order to minimize the scrap material. Square and rectangular cells can be a valid choice concerning planar configuration. Tubular cells also represent a good alternative in order to optimize manufacturing processes. A techno-economic key point in SOC devices is represented by auxiliary units dedicated to the reactants pre and post processing. Stack design has to take into account auxiliaries issues and during design trade off processes the interaction between all devices has to be considered. The ideal stack shouldn't need any other chemical devices and has to provide power output (voltage and current) considering the power conditioning devices needs. Improvements in solid oxide cell materials have of course a crucial impact in order to reach this configuration especially concerning the reactant processes. and some prescriptions can be considered in order to minimize the influences in term of interactions and in term of costs of the auxiliaries.

The last SOC techno-economic issues are related to manufacturing processes and advanced treatments concerning the other components of the stack (metal parts, insulating, superficial treatments, sealing, etc…). Planar configuration is characterized by very thin metal plates and geometric characteristic lengths that require high accuracy in term of manufacturing tolerances and advanced technological processes. The conjunction of this two aspects (high accuracy in manufacturing and complex parts shapes) has an huge impact in term of production costs. Furthermore critical thermal issues can emphasize any criticisms or defects of the components. On the other hand tubular configuration is characterized by bigger characteristic lengths and requirements in term of tolerances are less stringent. Simpler stack geometry shapes and lower accuracy in manufacturing processes can dramatically reduce the costs related to the metal and other accessory parts.

All this considered it is possible to summarize the SOC stack specifications also taking into account considerations presented in Chapter 2 for SOEC operating mode:

- operating temperature has to be increased at least up to 1000 °C;

- high current density has to be considered in order to maximize the power density of the stack;

- in order to use the stack both in SOFC and SOEC operating mode the SOC stack has to work always in exothermal mode that implies high SOEC voltage (high current density) to overcome the thermo-neutral point, as discussed later (see Figure 1);

- in SOFC operating mode current density has to be reduced in order to maximize the efficiency and to obtain similar thermal conditions respect to SOEC operating mode;

- reactants utilization has to be maximize to improve the overall device efficiency independently by the operating mode;

- stack design has to be cell-independent (cell thickness, cell performances, cell materials, etc…) to be coupled with different cells following the innovations produced by cells research;

- materials and manufacturing processes of the stack have to be simpler as possible in order to minimize the related capital costs;

- stack assembly procedure has to be designed in order to simplify the assembly process and to handle any imperfections in robust way;

- stack design has to provide homogeneous operating conditions to the cells in order to reproduce ideal conditions as much as possible.

Considering the operating point in SOFC and SOEC configurations, it has to be stressed that the main constraint for the reversible operation is the thermal invariance of the device. As the operating point is selected concerning thermal standpoint and the cell and stack losses are fixed, the SOFC and SOEC operating points are unequivocally related. In particular in SOEC operating condition high current densities are reached because the thermal neutral voltage has to be overcome. In SOFC operating condition low current densities are obtained and this maximizes the efficiency. In Figure 1 is shown a schematic representation of the relation between reversible operating points.
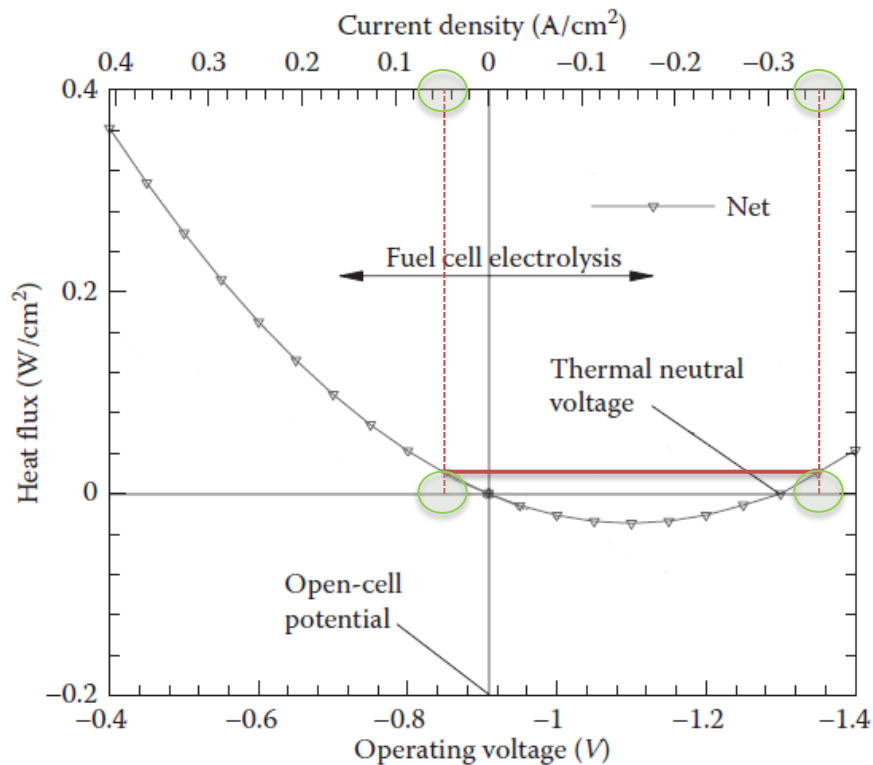
Figure 1: Schematic view concerning the operating point in reversible operating conditions (4)

In particular the most important trade off in SOC stack design is between efficiency and reliability. Now day in general higher priority is given to the efficiency, especially concerning SOFC, and this has favored the planar configuration. The drawback of this choice is that until now the reliability and the durability of SOC stack don't reached yet acceptable values for the market. One of the main motivation to privileging the

efficiency of the devices is related to the need to provide better performances respect to actual technologies. The author opinion is that SOC devices can't only replace the same functions provided by other devices based on different technology but they can have to be implemented in other innovative scenarios and have to satisfy additional needs. This lead to privilege the devices durability instead of devices efficiency. Once the reliability is reached technology improvements can be done in order to increase the efficiency also and to compete with traditional devices and technologies in their reference markets. In fact at the present days the major obstacle in SOC investments and market penetration is due to the too short devices life that make impossible to redact business plans in accurate way (5).

Innovative design

In the previous paragraph the key points of the state of the art in SOC technology have been described and the specifications for a novel stack are been derived. In the present paragraph a new SOC stack architecture is presented describing both the overall configuration and single components.

Now days tubular configuration was de facto abandoned in favor of planar configuration. Planar configuration could certainly be the future in the SOC technology but according to the author opinion tubular configuration has to be take in into account until the solid oxide cells technology reaches the maturity especially concerning SOEC applications. In fact one of the major key characteristic of the planar configuration is the high efficiency that can be reached. But planar devices are characterized by complex geometry and requires high tolerance levels in term of manufacturing and this has an impact both on capital costs and on durability. Furthermore planar stacks are more rigid and transmit higher stresses to the cells. This is the motivation that justifies the tubular configuration on the novel stack architecture. Micro SOC (6) are not taken in into account because even if they have good qualities in term of stack design they still have strong manufacturing tolerance needs.

Stack overall description

The novel stack Single Repeating Unit (SRU) is characterized by an autonomous and independent design. Many SRU can be linked in series or in parallel in order to reach de desired voltage-current operating point considering the other electronic devices specifications. An overview of the SRU in shown in Figure 2.
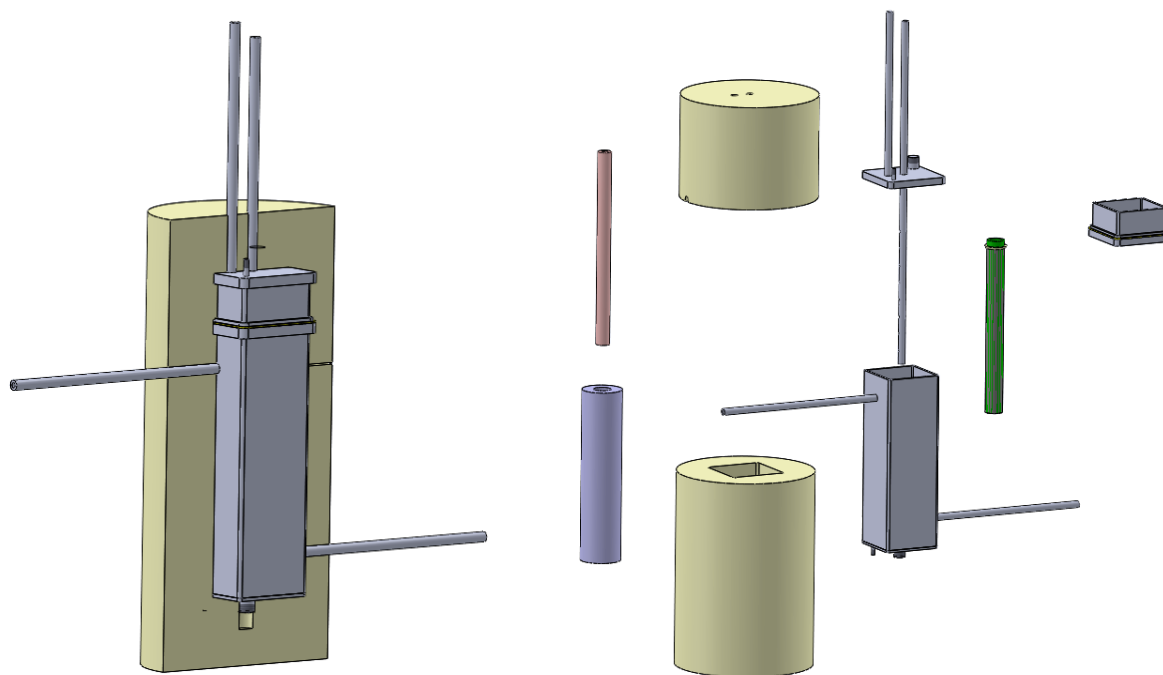
A rigid insulating encloses the metal main body with overall external sizes of 55 by 55 mm (in plane size) and 200 mm (stack eight) as shown in Figure 5. The external-lower part of the stack is related to the air side and the fluid (air) flow enters from the bottom right tube and exits from the top left tube (Figure 2). The inner-upper part is related to the reactants side where nickel-catalyzed reactions occur. The reactants enter from the top central tube. Before exiting, the exhausts pass through a chamber and conveys to the outlet tube placed in the top of the stack. The design of the stack has a symmetry plane in order to facilitate the multi SRU architecture. The only exception is represented by the main inlet tube that presents a swirling geometry in order to improve the reactants distribution.

The cell is a tubular cathode (SOEC) supported cell with closed end. The cell diameter is equal to 17 mm while cell length is equal to 150 mm with an active length equal to 130 mm. The bottom part of the cell can either be covered by the printed anodic electrode or only with the printed electrolyte. During the stack

development also a common tubular cell with both ends opened had be taken in into account. In this case a ceramic tap with truncated cone shape has be considered and the connection between the tap and the cell has to be made by the same main sealing used to join the cell and the metal plates. This solution has to be considered only if it can contribute to reduce the cells manufacturing costs.

Electric connections between electrodes and the external current collector are realized by metallic foams. In this way the charge carrier paths inside the electrodes are minimized. In common tubular cells with diameter d and thickness t the mean path length of the charge carriers is equal to $t + \frac{1}{4}\pi d$. In the new proposed stack configuration the mean path is simply equal to t similar to planar configuration. The inner foam is placed inside a reducing environment and no particular issues are remarked. Contrary the external foam is placed in an hard oxidizing environment that compromises the foam functionality. Coating deposition of the foam can't be considered because the shape of the foam and the wires overlapping make it impossible to realize. The solution here proposed consists in the coating deposition of the foam wires before the foam manufacturing. In this way all the area of the foam can be covered and performance of the foam can kept high during all SOC life cycle. The air side foam is recognized as the most critical element inside the stack and the design of the assembly in term of maintainability has been studied in order to permit the substitution of that foam.

A stack section view is shown in Figure 3 with some descriptions. Considering notations there proposed the air and reactants flow path are now described.

1. Air path:
    a. the air enters from the inlet tube on the right;
    b. air reacts at electrode proximity and passes through the air side foam;
    c. air exits from the outlet tube on the left.
2. Reactants path:
    a. reactants enter from the top central inlet tube;
    b. reactants diffuse in the conductive foam and reacts at electrode proximity;
    c. a compensation chamber collects the exhausts;
   d. the exhausts exit from the outlet tube.
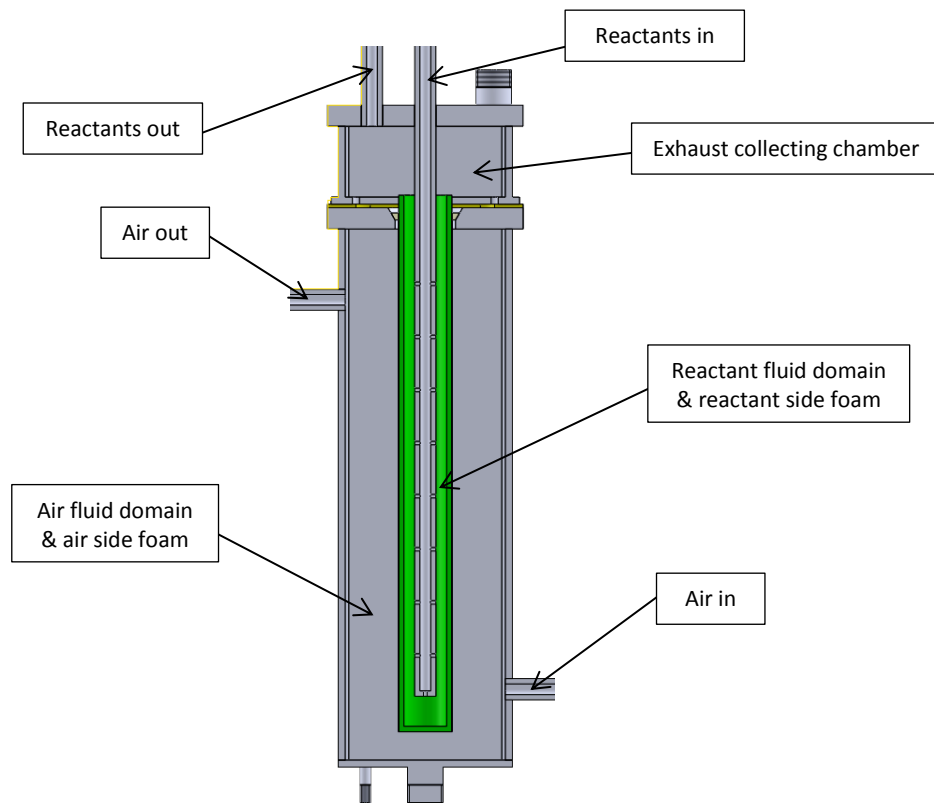
Figure 3: Section view of the SOC stack

In Figure 4 the exploded view of the SOC stack is shown with the bill of materials. As can be derived from the exploded view the different components are been grouped in three main independent sub-assembly. This helps the manufacturing and the procurement process in general. In Figure 5 the executive technical drawing is reported emphasizing the overall dimension of the SRU.

It has to be specified that the novel design proposed has some peculiarities that are not related to specific sizing. The scale up of the stack is supposed to be obtained coupling many SRU as usual. Anyway different cells can be adopted in the single SRU in order to fit particular needs in term of voltage and power or to match some economic constraints.

68
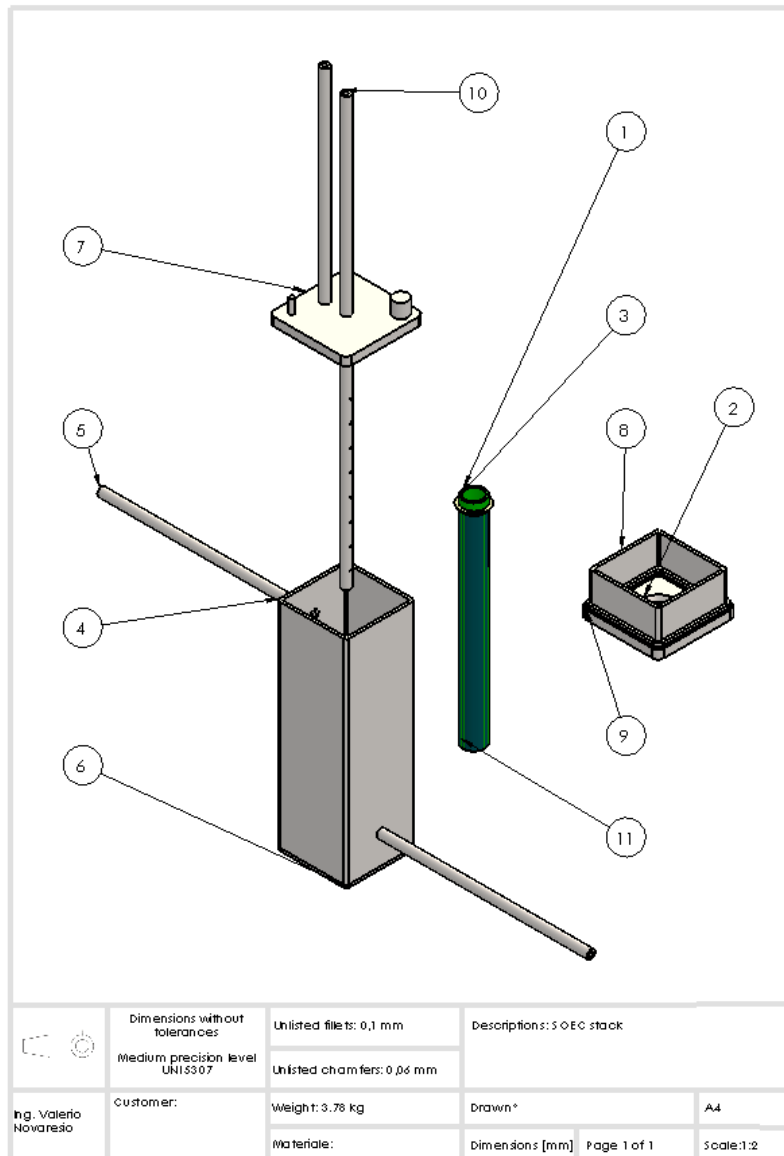
Num. articolo	Num. parte	Quantità
1	Fuel side cell	1
2	Sealing plate	1
3	Sealing	1
4	Stack body	1
5	Inlet/outlet tube	3
6	Ending plate	1
7	Superior plate	1
8	Superior body stack	1
9	Mica insulating	1
10	Inlet fuel tube	1
11	Oxidant side electrod	1

Figure 4: Stack assembly technical drawing and related BOM
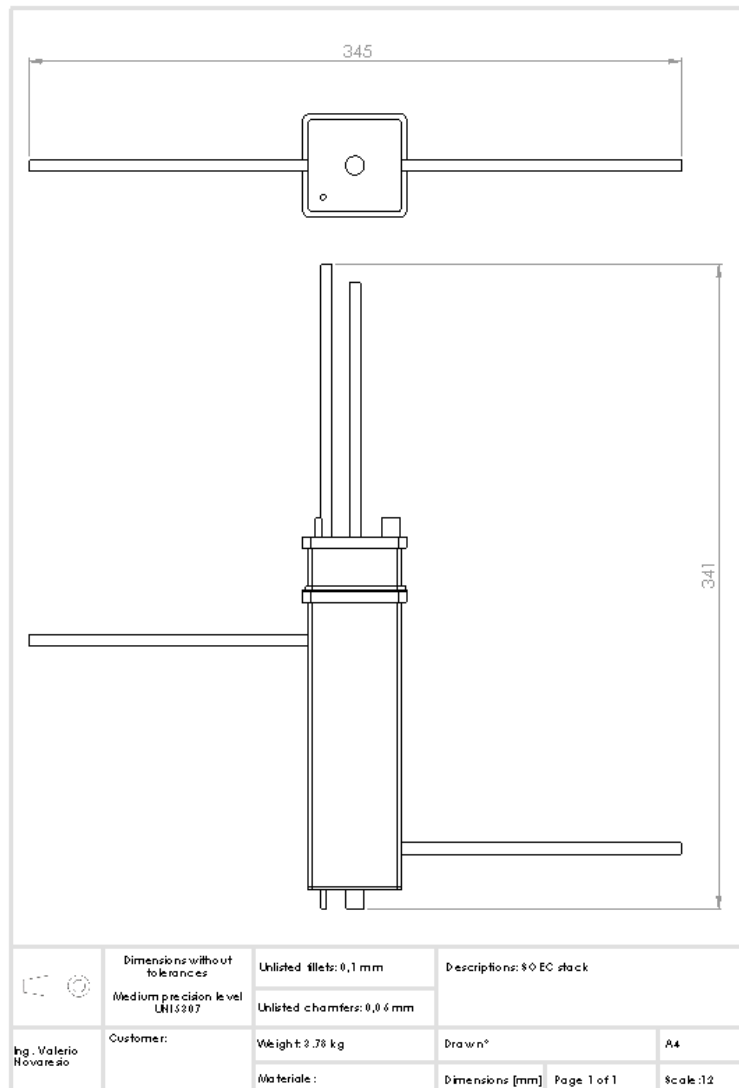
Figure 5: SOC technical drawing with overall dimensions

Stack components description

In this paragraph a brief description of the metal components is provided. For each element some details concerning manufacturing are also reported. The material considered is the stainless steel 1.4762. In order to minimize the impact of the metal parts on the global cost of the stack no special steels are taken into account. This steel has been chosen for is compatibility in term of thermal deformation with cells materials and sealing as reported in Table 1. Common steel has been considered supposing that the durability of the stack is guaranteed by a superficial coating treatment.

Stack main body

The main metal element of the stack is the metal housing. It is obtained from a square profiled stainless steel with 2 mm thickness. Two holes are obtained in opposite side for the air inlet and outlet tubes. In Figure 6 executive drawing is reported. Internal superficial treatment or coating deposition has to be considered in order to minimize the air electrode poisoning due to metal volatile compounds.
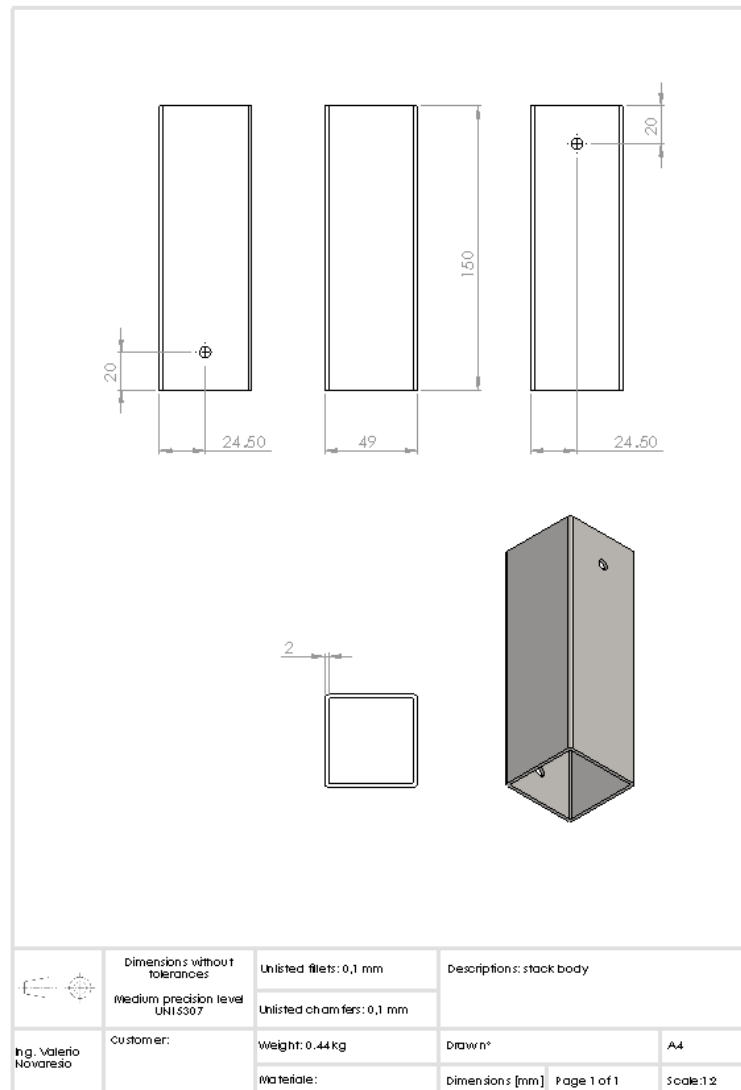

Figure 6: Stack main body executive technical drawing

Stack top body

The secondary metal element of the stack is the superior housing. It is obtained from a square profiled stainless steel. At the bottom of the body a 6 mm shoulder is present in order to increase the contact area between the metal part and the insulating mica sheet. It can be obtained by solid molding or simply welding the shoulder with the profiled. Considering the second manufacturing approach in this component scraps are produced. Figure 7 shows the top body technical drawing.
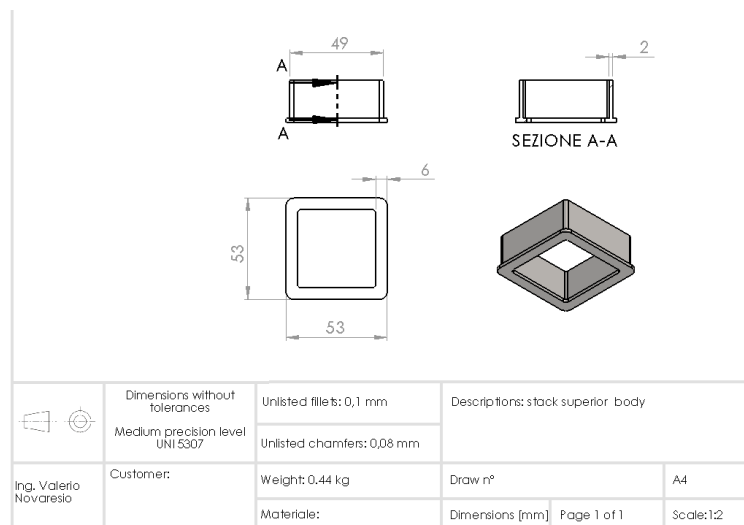
Figure 7: Stack superior body executive technical drawing

Sealing plate

The sealing plate is obtained from a 6 mm stainless steel metal sheet. Manufacturing scraps are produced in order to smooth the plate corners. In the plate center a countersunk hole is present. It is obtained by a preliminary hole machining followed by punching processes. In Figure 8 part technical drawing is shown. Countersunk hole is design in order to facilitate the sealing processes. The cold viscous sealing can be casted in the interspace between the hole and the cell without leaching. During the heat up process and sealing transition it can adapt its shape in order to occupy the optimal volume. The sealing plate and the cell forms one of the sub-assembly of the stack.
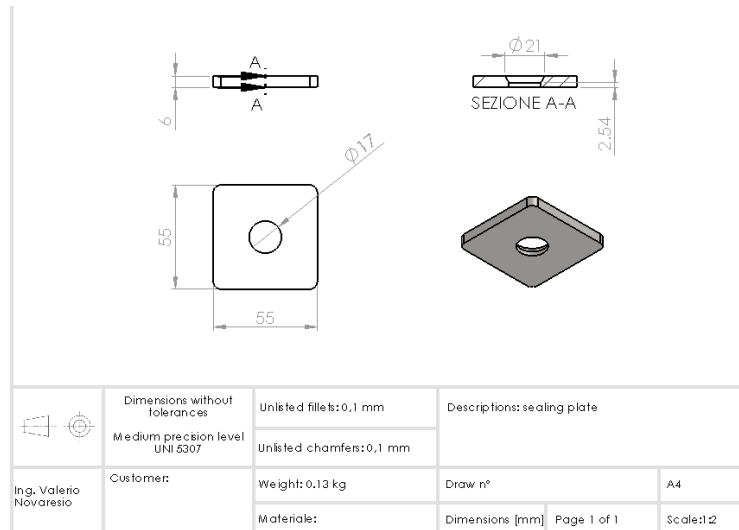
Figure 8: Stack sealing plate executive technical drawing

Top plate

The top plate is obtained from a stainless steel metal sheet. Manufacturing scraps are produced in order to smooth the plate corners. On the plate two holes are present for the reactants inlet and outlet tubes. On the top side current and voltage takes are obtained by welding two threated bars. Alternatively the part can be obtained by machinery in order to avoid the welding of the electric takes. This can improve the performances and can reduce the contact losses between metal parts but this solutions produce high quantity of manufacturing scraps and requires longer manufacturing times having bad influence on costs. Figure 9 shows the technical drawing of the component.

	Dimensions without tolerances	Unlisted fillets: 0,1 mm	Descriptions: superior plate		
	Medium precision level UNI 5307	Unlisted chamfers: 0,1 mm			
Ing. Valerio Novaresio	Customer:	Weight: 0.15 kg	Draw n°		A4
		Materiale:	Dimensions [mm]	Page 1 of 1	Scale:1:2
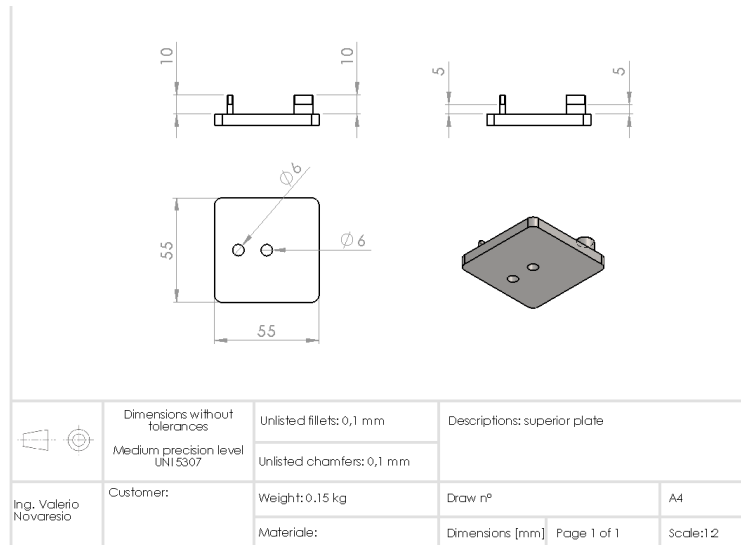
Figure 9: Stack top plate executive technical drawing

Ending plate

The ending plate represents the bottom part of the stack. It is a similar component respect to the superior plate. The only difference between the two plates is the absence of the holes in this part. Figure 10 shows the technical drawing of the bottom plate.

	Dimensions without tolerances	Unlisted fillets: 0,1 mm	Descriptions: ending plate		
	Medium precision level UNI 5307	Unlisted chamfers: 0,1 mm			
Ing. Valerio Novaresio	Customer:	Weight: 0.05 kg	Draw n°		A4
		Materiale:	Dimensions [mm]	Page 1 of 1	Scale:1:2
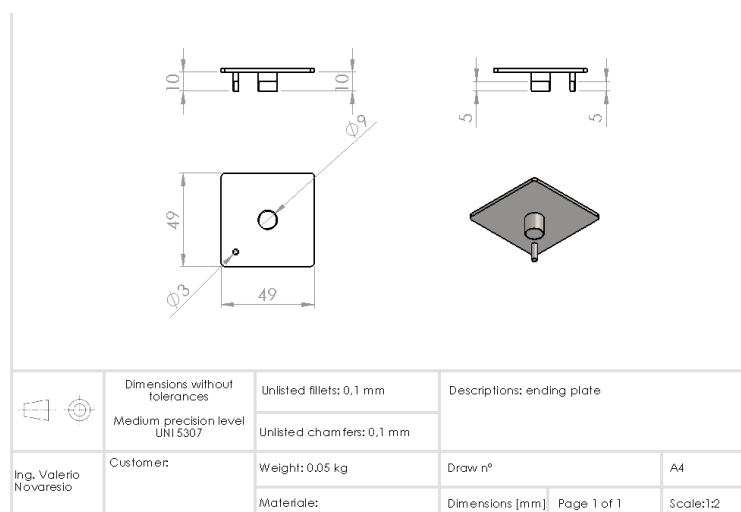
Figure 10: Stack bottom plate executive technical drawing

Reactants inlet tube

The reactants inlet tube is a stretched stainless steel tube with an inner diameter of 3 mm. The tube thickness is equal to 1.5 mm in order to provide relevant strength useful both for operating condition and for manufacturing processes. The tube presents a bottleneck at the end with a diameter of 1 mm. On the tube side an helicoidally series of 1 mm holes are obtained in order to gradually distribute the reactants inside the stack. In Figure 11 the technical drawing of the tube is shown. The sizing of the holes diameter is obtained performing a parametric Design Of Experiment (DOE) considering the reactants utilization as the cost function to be maximize. Parametric study has been done also for the ending bottleneck. In this case greater sensitivity was observed and this sizing is one of the more critical parameter in the stack design.
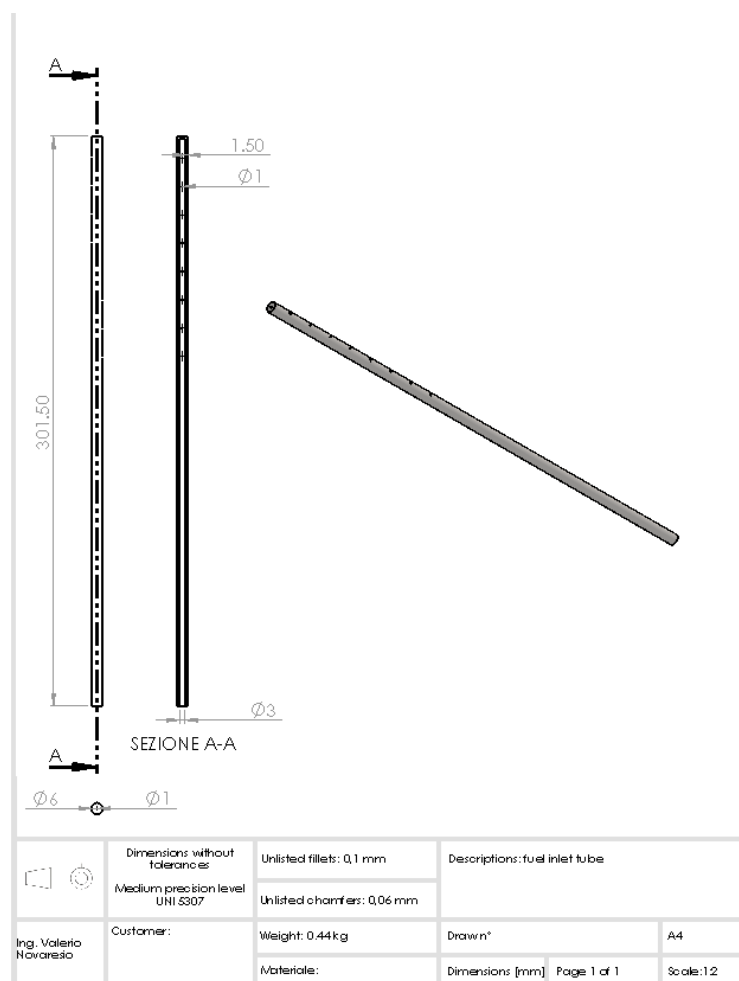

Figure 11: Reactants inlet tube executive technical drawing

Assembly procedures

The assembly procedure prescribes that three separate sub-assemblies have to be built, one for the reactants side part, one for the air side part and the third for the cell and the sealing plate. The stack main body has to be welded with the bottom plate and with the air inlet and outlet tubes. As the assembly is built the conductive foam has to be put inside, leaving the necessary cylindrical space for the cell. As a general rule the foam inner diameter has to be 2 mm smaller than the cell diameter in order to have interference fit during the assembly. Parallel the stack top body has to be welded with the top plate and with the reactants inlet and outlet tubes.

The most complex part of the assembly procedures concerns the sealing plate. As described in the previous paragraph the sealing plate and the cell are joint with a glass ceramic sealing. The sealing is deposited in viscous paste form and has to be heated up in order to sinter. This process has to be done separately by the rest of the assembly and represents the bottleneck of the entire procedure. The sealing sintering can done also directly during the global stack eating up reducing the time and costs of the assembly but considerably increasing the risks to obtain high percentage of non-conformal product. Inside the cell a conductive foam has to be inserted in, leaving the necessary cylindrical space for the reactants inlet tube. After the thermal treatment is completed the assembly composed by the sealing plate and the cell become an unique part and this has to be overall substitute in case of maintenance.

Once the three sub-assemblies are built they have to be mounted together simply putting combining them. Between the sealing plate and the top part an insulating mica sheet has to be inserted in order to electrically separate the two SOC side. At the end two cylindrical insulating housings have to be mounted over the stack. The tightening is done out of the insulating in order to preserve the threaded links from the high temperature. Bolted junctions are design to operate at low temperature in order to be removable. Bolts transmit the compression load to the rigid insulating parts and finally to the stack metal housing. In order to pander SOC stack tolerances and shifts due to thermal expansions an elastic element is interposed between each bolted junctions.

Fluid dynamic numerical simulations

In order to estimate the novel SOC stack design improvements some simulations have been set up. Using the in-house developed solver presented in Chapter 3 complete polarizations both in SOFC and SOEC mode are performed. Two verification criteria are been individuated:

- the capability to handling high reactants utilization;
- the current density distribution in high reactants utilization operating conditions.

Figure 12 (a) shows the water vapour distribution inside the stack in SOEC operating conditions. The relevant operating data are reported in the same figure (b). In this case reactant (water) utilization of 95% is reached. Thanks to the foams, without any obstacles (solid pins or ribs) the stack can auto-equilibrate the reactants consumption and distribution. Current density profile is continuous even if it is not homogeneous as shown later on. The absence of solid pins or ribs implies the absence of "checkerboard discontinuity" in term of current density and in term of induced thermal stresses favoring the durability of the device.

Data type	Value
Inlet condition (molar fractions)	$H_2 = 2\%$
	$H_2O = 98\%$
	$O_2 = 21\%$
	$N_2 = 79\%$
Geometry description	Novel SOC stack design
Temperature	1000 °C
Operation mode	SOEC

(a)   (b)
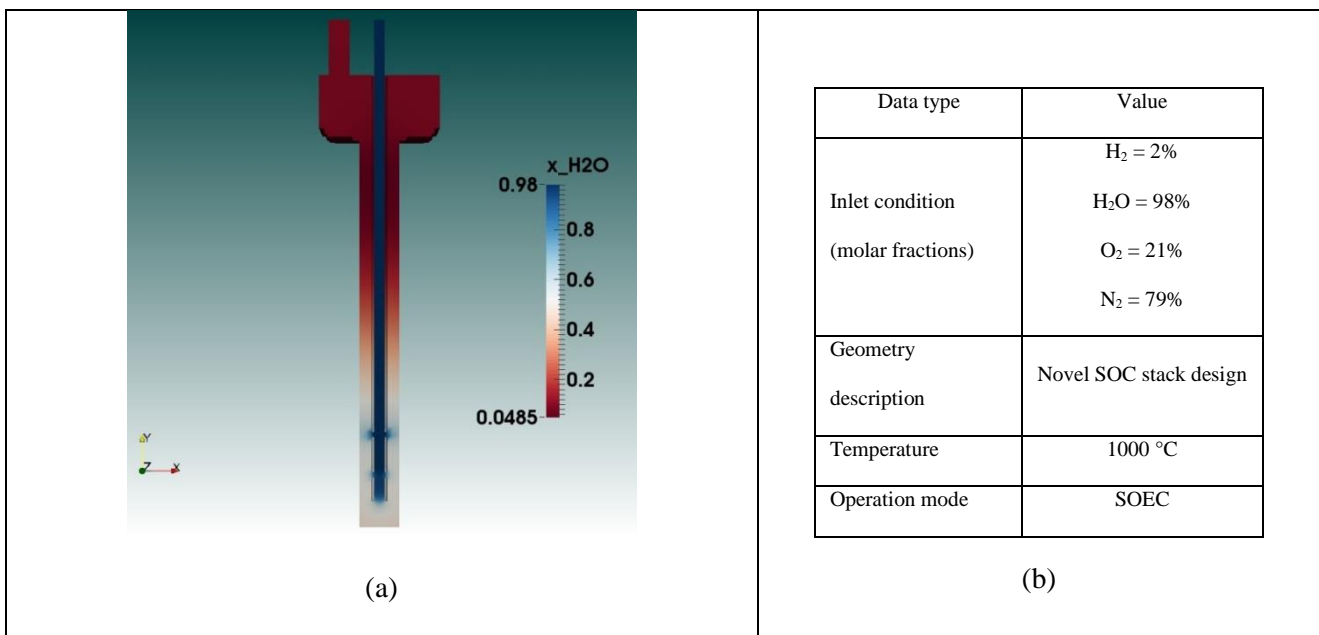
Figure 12: Water molar fraction in SOEC high reactants utilization operating condition (a) and table with the main operating conditions (b)

Similar considerations can be done in SOFC operating condition where very high fuel utilization can be reached as shown in Figure 13.

| Data type	Value
Inlet condition (molar fractions)	$H_2 = 97\%$
	$H_2O = 3\%$
	$O_2 = 21\%$
	$N_2 = 79\%$
Geometry description	Novel SOC stack design
Temperature	1000 °C
Operation mode	SOFC

(a)

(b)
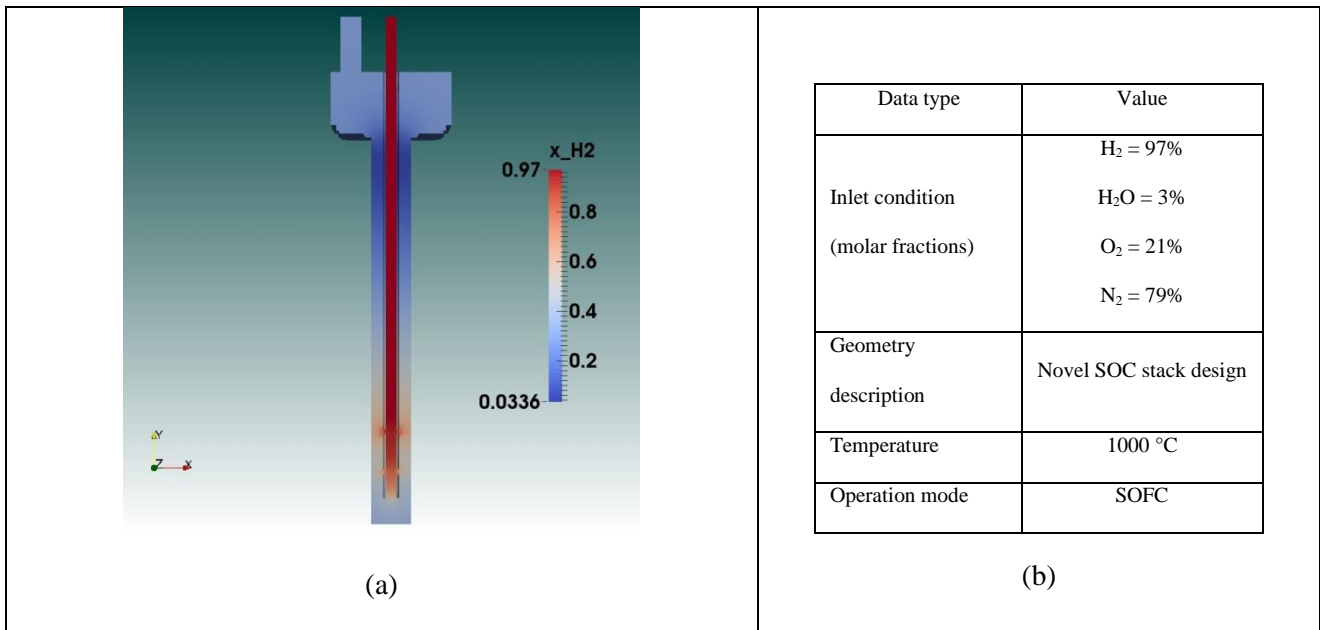
Figure 13: Hydrogen molar fraction in SOFC high reactants utilization operating condition (a) and table with the main operating conditions (b)

The second relevant results is concerning the current density distribution along the cell. Is well known that if external load is applied and if there is a finite flow field distribution (from inlet to the outlet) some inhomogeneity in physical quantities appear (especially reactants and current density). The more is reactants utilization the more the inhomogeneity increases. Solid obstacles (pin/ribs) emphasize these critical aspects. The best current density profile is related to low reactants utilization configuration. In order to analyze the performances of the novel SOC stack design the current density profile has been calculated along the direction line shown in Figure 14. Results are shown in Figure 15 for different SOFC and SOEC operating conditions. The two reference cases are the ones characterized by low reactants utilization conditions. The common shape of the current density distribution is characterized by a central point where the current density tends to zero. This is due to the particular reactants injection strategy and variations are limited between different operating conditions. With the novel stack design the current density variations along the cell are considerably limited and in first approximation there are no differences between low and high reactants utilization configuration, both in electrolysis mode and in fuel cell mode. The maximum level of the current density inhomogeneity is equal to 25% in SOEC operating mode and 30 % in SOFC operating mode. One of the most relevant results is that the variations between two adjacent points on the electrolyte are very limited as can be deduced from Figure 15.
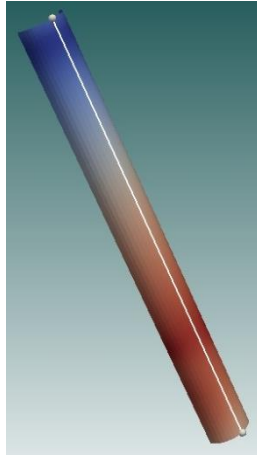
Figure 14: plot line to evaluate current density profile performances

High oxygen
molar fraction

High reactants
molar fractions

Zone where equilibrium
potential is equal to the
applied voltage

SOFC low RU   SOFC high RU   SOEC low RU   SOEC high RU
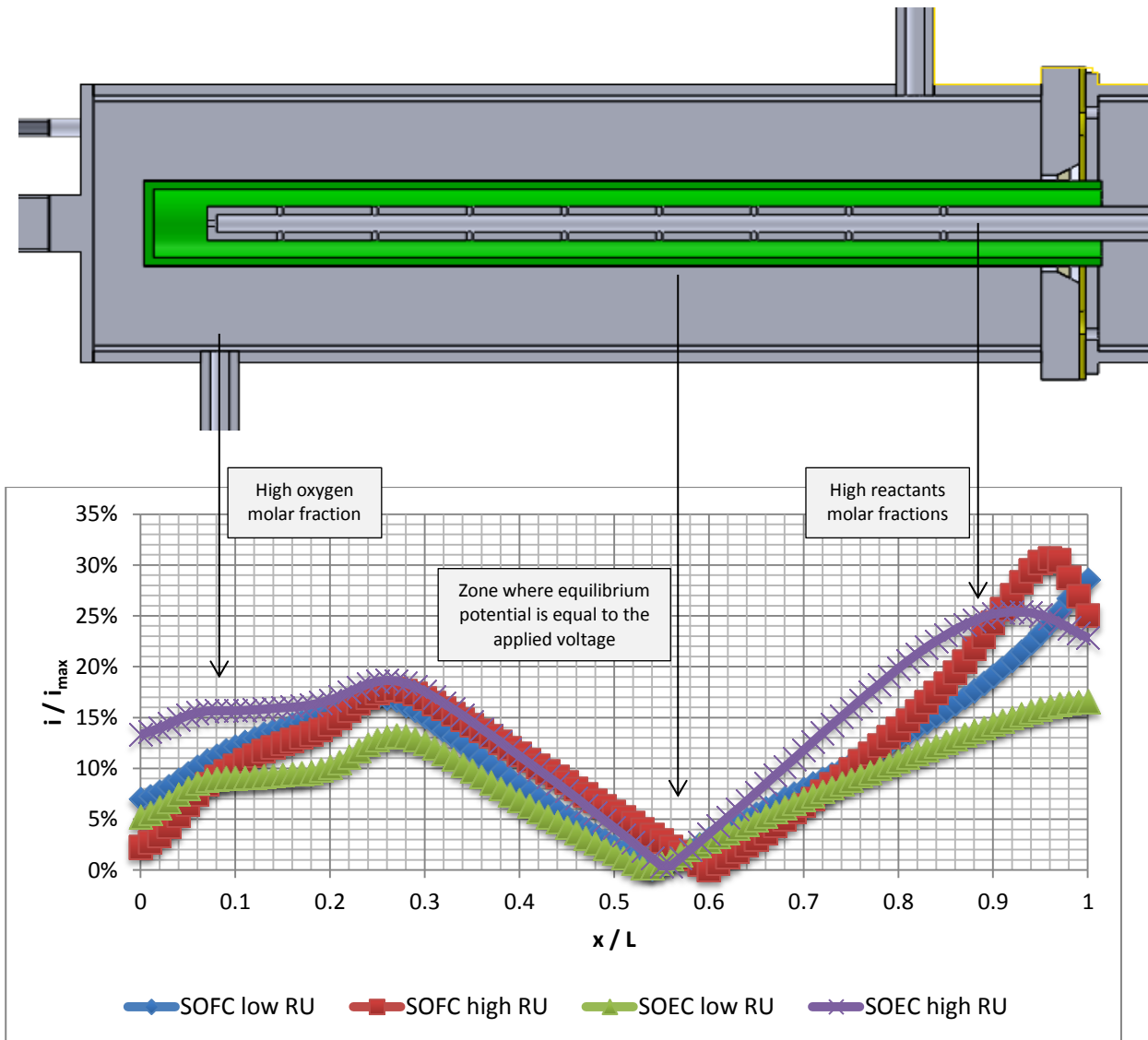
Figure 15: current density profile in different SOFC and SOEC operating conditions

Structural numerical simulations

As a consequence of the good current distribution along the cell the temperature field likewise shows good distribution also. This effect combined with geometrical improvements related to the cell and metal part shapes significantly influences the structural performances. In order to show these improvement a verification criterion concerning the mechanical stress at the cell-sealing-metal interface has been identified. A finite element model was developed in order to evaluate the stresses induced by thermal loads. First a numerical loop between the SOC fluid solver and solid parts thermal solver has been performed in order to reach the steady state solution. Then thermal field has been transferred to a Nastran NX® solver using the Femap® pre-processor (7). Relevant data of the simulation are reported in Table 1. Comparative analysis has been done between square planar configuration and the novel configuration and results are shown in Figure 16. Square configuration shows stress concentrations near cell corners (Figure 16 - a). These stress peaks combined with inhomogeneous current density (thermal load) and temperature distribution contribute to increase the creeks propagation and to reduce the useful life of the brittle materials and the SOC stacks in general. In the SOC novel stack design here proposed the thermal induced stress are considerably reduced favoring the reliability and the durability of the device (Figure 16 - b). Stress levels obtained in simulations are affected by uncertainties related to material properties at high temperature. Even considering there uncertainties the results show that the order of magnitude of the stresses in planar square configurations are similar to the common sealing tensile strengths. Contrary in novel stack design the sealing-metal and sealing-cell interfaces are essentially unloaded.

Data	Value
Metal modulus of elasticity [GPa]	$E_m = 155$
Cell support modulus of elasticity [GPa]	$E_c = 52$
Sealing modulus of elasticity [GPa]	$E_c = 72$
Metal coefficient of thermal expansion [10^{-6}/k]	$\alpha_m = 13.5$
Cell support coefficient of thermal expansion [10^{-6}/k]	$\alpha_c = 10.5$
Sealing coefficient of thermal expansion [10^{-6}/k]	$\alpha_s = 10.7$

Table 1: relevant data concerning FEM thermos-mechanical simulation (8)

(a)   (b)
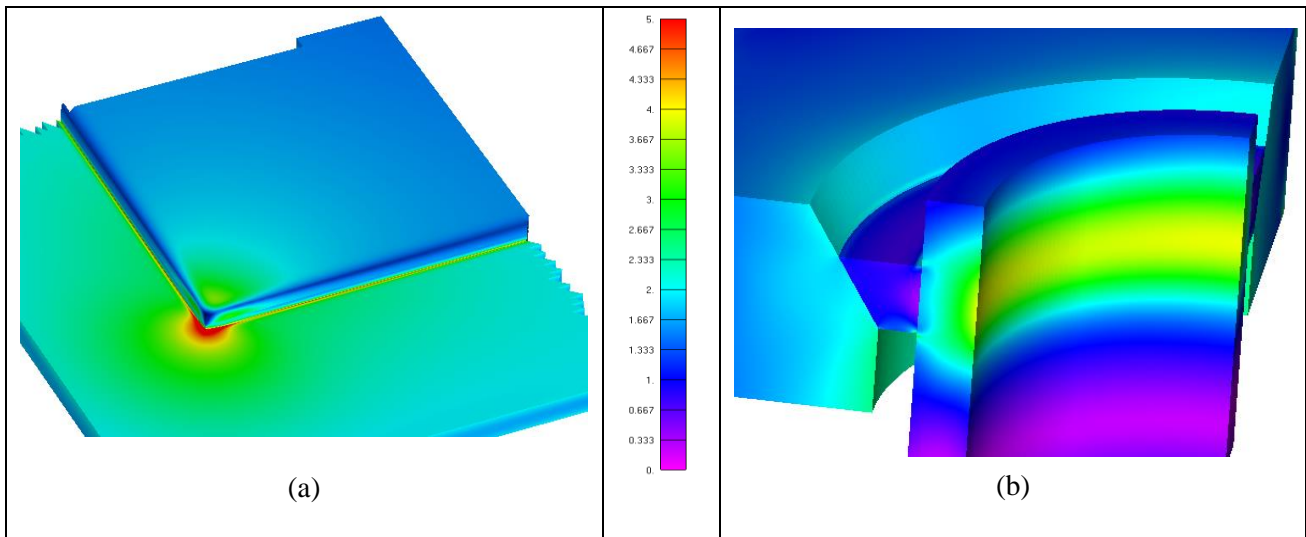
Figure 16: Comparison between thermal stresses in common planar configuration and novel configuration (stresses in MPa)

1. *FUEL CELLS – SOLID OXIDE FUEL CELLS | Overview.* **Singhal, X.-D. Zhou and S.C.** Amsterdam : s.n., 2009, Encyclopedia of Electrochemical Power Sources, p. 1-16. 9780444527455.

2. *Fabrication and characterization of low-temperature SOFC stack based on GDC electrolyte membrane.* **Jiao Ding, Jiang Liu, Guoqiang Yin.** 1–2, 2011, Journal of Membrane Science, Vol. 371, p. 219-225. 0376-7388.

3. *The cost of domestic fuel cell micro-CHP systems.* **Iain Staffell, Richard Green.** 2, 2013, International Journal of Hydrogen Energy, Vol. 38, p. 1088-1102. 0360-3199.

4. *Nuclear Idrogen Production.* s.l. : Yan, X., L., Hino, R., 2011.

5. **S.r.l., Acacia Cleantech.** Acacia Cleantech techno-economical review. Turin : s.n., 2013.

6. *The properties and performance of micro-tubular (less than 2.0 mm O.D.) anode suported solid oxide fuel cell (SOFC).* **Yong-Wook Sin, Kevin Galloway, Brycen Roy, Nigel M. Sammes, Jung-Hoon Song, Toshio Suzuki, Masanobu Awano.** 2, 2011, International Journal of Hydrogen Energy, Vol. 36, p. 1882-1889. 0360-3199.

7. Femap with Nastran NX. [Online] http://www.plm.automation.siemens.com/it_it/products/femap/nxNastran/.

8. *Glass–ceramic seal to join Crofer 22 APU alloy to YSZ.* **F. Smeacetto, M. Salvo, M. Ferraris, J. Chob, A.R. Boccaccini.** 2008, Journal of the European Ceramic Society, Vol. 28, p. 61–68.

Chapter 5
Conclusions

Concluding summary

Energy is the main driver of human evolution. Every improvement in people's life style during the history is associated to some new energy sources or to a development of a new smart way to use energy. As the population continuously increases, energy demand has grown up dramatically, especially during last decades. This yields to an huge increases of the inequality between peoples and nations. Moving on renewable sources is mandatory both concerning the sustainability of the energy demand and for reducing the influence of the geolocation of the sources.

Renewables energies are usually characterized by low power density and poor predictability. This aspect represents a mismatch respect to the energy constraints related to the present "modern" life style. In order to have energy "when we want" and "where we want", storage techniques have to be developed. Viability of a particular storage solution is evaluated as a tradeoff between sustainability, economic aspects and improvements in human life style. Unfortunately in present days the economic aspects have an (overestimated...) dominant role respect to all other aspects. Hence some storage solutions are not investigated enough or definitively abandoned only because they can't guarantee adequate profits.

According to author's opinion the main driver that has to be taken into account while approaching energy issue, is the ethical one. If a storage solution is ecologically sustainable there are no other reasons to hinder it. If it can be done it has to be done! Considering renewable energies as primary sources, efficiency plays only a secondary role.

- Conscious of these economic constraints, a storage solution, based on solid oxide electrolysis cell, has been evaluated. Some chains have been described and SOEC technology can be promising because it can adapt to different scenarios. Furthermore several market penetrations are possible depending on technology maturity and local energy framework. The new proposed design tries to taking into account three different needs:

83

- minimization of the capital cost, so the stack has to be constructively simple;

- minimization of the internal mechanical stresses and maximization of the damage tolerance in order to maximize the MTBF and the useful life of the device;

- capability of reversible operation in order to increase the adaptability of the device.

Furthermore the proposed design is completely technology-free respect to the new developments of solid oxide cells. All this features make this stack a good candidate to become the base layout for future SOEC devices.

Additional remarks, limitations and future prospects

The present PhD thesis tries to explain the work done to design a novel SOEC stack. Some key aspects have been shown, i.e. the in-house developed numerical solver, the pragmatic method used and the problem solving approach. Nevertheless, even if justified in the text, many features could have been analysed in more detailed way. The two main weaknesses of the thesis and of the PhD activities are:

- the missing of the prototype manufacturing and the consequent exhaustive experimental part;

- the full coupling between numerical solvers.

The second weaknesses is mainly related to the problem encountered with the robustness and reliability concerning the modeling of heterogeneous reaction mechanisms . Contrary the absence of the prototype manufacturing is due founds issues. Even if the stack is designed in order to be cheap too high funds are required for prototyping activity. Furthermore solid oxide cells producers are focused on planar configurations and there is no commercial availability of tubular cells designed as described in the text.

Concerning funds, the main modeling parts have been done using open source tools and when it was unfeasible (Femap® with Nastran NX® and SolidWorks®) the required software has been bought by the author with his own private funds.

As a comment of the PhD activities it is interesting compare the different point of view of the academia and the companies. The design activity has been done both in academic context (Polytechnic of Turin) and in industrial context (Acacia Cleantech S.r.l. – Spin off of the Polytechnic of Turin). The author was a co-founder of the company and during the activities it was unbelievable to see how the "profits mantra" poisons the research. According to the religion of the profit only thighs that can guarantee profits have to be considered and developed. Usually it is considered that the academic world is too far from industrial world and many efforts are spent in order to reduce the gap. According to the author opinion this sentence is only in part true because it is wise and better to say that the industrial world is too far from academia world.

The last remark concerns the regret to have analysed the stack, the design and the different solutions from the economic standpoint, according to common technical literature, even if the author is perfectly conscious that these aspects are definitely the less relevant ones.